

## Geographic and temporal variability in Pleistocene lion-like felids: Implications for their evolution and taxonomy

Martin Sabol, Adam Tomašových, and Juraj Gullár

### ABSTRACT

Several taxa of lions occurred in the Pleistocene of the Northern Hemisphere. Although crania of these large cats are relatively rare in the fossil record, they allow us to assess size and shape differences among Pleistocene lions from Europe, Asia, and North America (*Panthera fossilis*, *P. spelaea*, *P. atrox*) and to compare them with the extant *P. leo*. We use basic 14 morphometric data (cranial length/width dimensions, auditory bulla diameters, cranial profile) including data on sex and ontogenetic age in 44 fossil and eight recent specimens, along with their geological age and altitude. We show that: first, crania of the *P. fossilis* (including *P. "intermedia"*) differs from crania of the Last Glacial *P. spelaea* and the extant *P. leo*. Second, *P. spelaea* shows a high morphologic variation in cranial morphology across its geographic range, with partial morphological segregation between the Western European and Eastern European assemblages. However, the main axis of morphological variation between geographic forms of *P. spelaea* and *P. fossilis*–“*intermedia*” correlates with size (in contrast to major differences relative to *P. atrox*), and cranial data thus do not consistently differentiate between these geographically and temporally-separated forms. These forms probably represent ecologically-differing geographic populations of the same chronospecies rather than distinct species. Geographic differences are driven by allometry, although other traits such as the teeth may allow their separation in the future analyses. However, the relationships in cranial morphospace still reveal geographic relatedness among subspecies: *P. spelaea* assemblage from the Western Europe is very similar to *P. fossilis*–“*intermedia*”, and contrasts with *P. spelaea* from the Eastern Europe and Asia. On one hand, such patterns suggest that the western *P. spelaea* is more related to *P. fossilis*–“*intermedia*” lineage and the eastern *P. spelaea* is related to individuals from Siberia. On the other hand, the similarity between the West-European specimens of *P. spelaea* (as immigrants from the East) and specimens of *P. fossilis*–“*intermedia*” can reflect functional convergence to similar environmental and climatic conditions prevailing in Western Europe.

Final citation: Sabol, Martin, Tomašových, Adam, and Gullár, Juraj. 2022. Geographic and temporal variability in Pleistocene lion-like felids: Implications for their evolution and taxonomy. *Palaeontologia Electronica*, 25(2):a26. <https://doi.org/10.26879/1175>  
[palaeo-electronica.org/content/2022/3681-lion-cranial-variability](http://palaeo-electronica.org/content/2022/3681-lion-cranial-variability)

Copyright: August 2022 Society of Vertebrate Paleontology.

This is an open access article distributed under the terms of the Creative Commons Attribution License, which permits unrestricted use, distribution, and reproduction in any medium, provided the original author and source are credited.  
[creativecommons.org/licenses/by/4.0](http://creativecommons.org/licenses/by/4.0)

Martin Sabol. Department of Geology and Paleontology, Faculty of Natural Sciences, Comenius University, Ilkovičova Str. 6, SK – 842 15, Bratislava, Slovak Republic, martin.sabol@uniba.sk

Adam Tomašových. Earth Science Institute, Slovak Academy of Sciences, Dúbravská cesta 9, SK – 840 05, Bratislava, Slovak Republic, geoltoma@savba.sk

Juraj Gullár. Reconum – Gullár, Muškátová 32, SK – 821 01, Bratislava, Slovak Republic, gullar.rekonum@zoznam.sk

**Keywords:** *Panthera fossilis*; *Panthera spelaea*; *Panthera atrox*; *Panthera leo*; Pleistocene; cranial morphology

Submission: 2 July 2021. Acceptance: 28 July 2022.

## INTRODUCTION

Lions (or lion-like felids) form a group of large pantherine cats comprising the extant species (*Panthera leo*) and its Pleistocene close relatives from the Northern Hemisphere, such as cave lion or American lion. The phylogenetic relationships of these felids and their taxonomic ranking are, however, still controversial and not well resolved. Morphological studies supplemented by molecular data in the past decades have provided support for both the species model (Terzea, 1965; Vereshchagin, 1971; Wiszniewska, 1978; Baryshnikov and Boeskorov, 2001; Sotnikova and Nikolskiy, 2006; Ovodov and Zaika, 2008; Barnett et al., 2009, 2014, 2016; Christiansen and Harris, 2009; Mazák, 2010; Stuart and Lister, 2011; Ersmark et al., 2015; Chernova et al., 2020; Stanton et al., 2020) and the subspecies model (Boule, 1906; Kurtén, 1968, 1985; Hemmer, 1967, 1974; Schütt, 1969; Schütt and Hemmer, 1978; Turner, 1984; Gross, 1992; Burger et al., 2004; Bona, 2006; Diedrich, 2008, 2009, 2011a, 2011b, 2011c; Schouwenburg et al., 2009; Baryshnikov and Tsoukala, 2010; Diedrich and Rathgeber, 2012; de Manuel et al., 2020). In addition, lions with their enormous Pleistocene geographic distribution from Africa through Eurasia up to America show relatively great morphological differences between regions. This is also reflected in certain morphological variations, which may not only be intraspecific variability, but may also be a manifestation of interspecies differentiation. These variations are observed in both dental and cranial morphology (Hemmer, 1974; Yamaguchi et al., 2004; Sotnikova and Nikolskiy, 2006; Barycka, 2008; Mazák, 2010).

Although crania of lion-like felids are relatively rare in the fossil record, some specimens are relatively well-preserved. This enables allometric and multivariate analyses that can be used to assess morphological differences between groups from different regions and stratigraphic units. In our

analyses, using basic morphometric data, such as cranial length/width dimensions, auditory bulla diameters, and cranial profile, we assess: 1) whether taxa identified to species level and assigned to *P. fossilis* (steppe lion), *P. spelaea* (cave lion), *P. atrox*, (American lion) and *P. leo* (extant lion) on the basis of non-cranial morphological characters can be discriminated on the basis of cranial characters, and 2) whether some morphological differences among these extinct and extant lion-like felids from Europe, Asia, Africa, and North America can be rather explained by differences in ontogenetic stage, sex, altitude, or stratigraphic age of specimens. Specifically, to assess whether the morphological variability in the cranium of lions can resolve their evolutionary and biogeographic history in response to environmental and climate changes, we evaluate whether craniometric variation in lion crania can discriminate between: 1) the steppe lion and the cave lion; 2) the Western and Eastern European forms of the cave lion; 3) the cave lion and the modern lion, and 4) whether the American lion overlaps with European and Asian extinct lions. Our analyses are based on traditional morphometric measurements and estimate bivariate allometric coefficients of several variables regressed on the log-transformed cranial length, multivariate (principal coordinate) analyses, and analyses of cranial profile angles.

## STATE OF ART

Based on craniometric (and partly also dental) characters, three to four distinct species of lions are traditionally distinguished, which is partly consistent with the results of some more recent molecular and paleogenetic analyses (Ersmark et al., 2015; Stanton et al., 2020) (Figure 1). In this model, the extant lion species represents a lineage that diverged from lineage(-s) of extinct lions during the early Pleistocene, while the cave lion and the American lion evolved from *P. fossilis* prob-

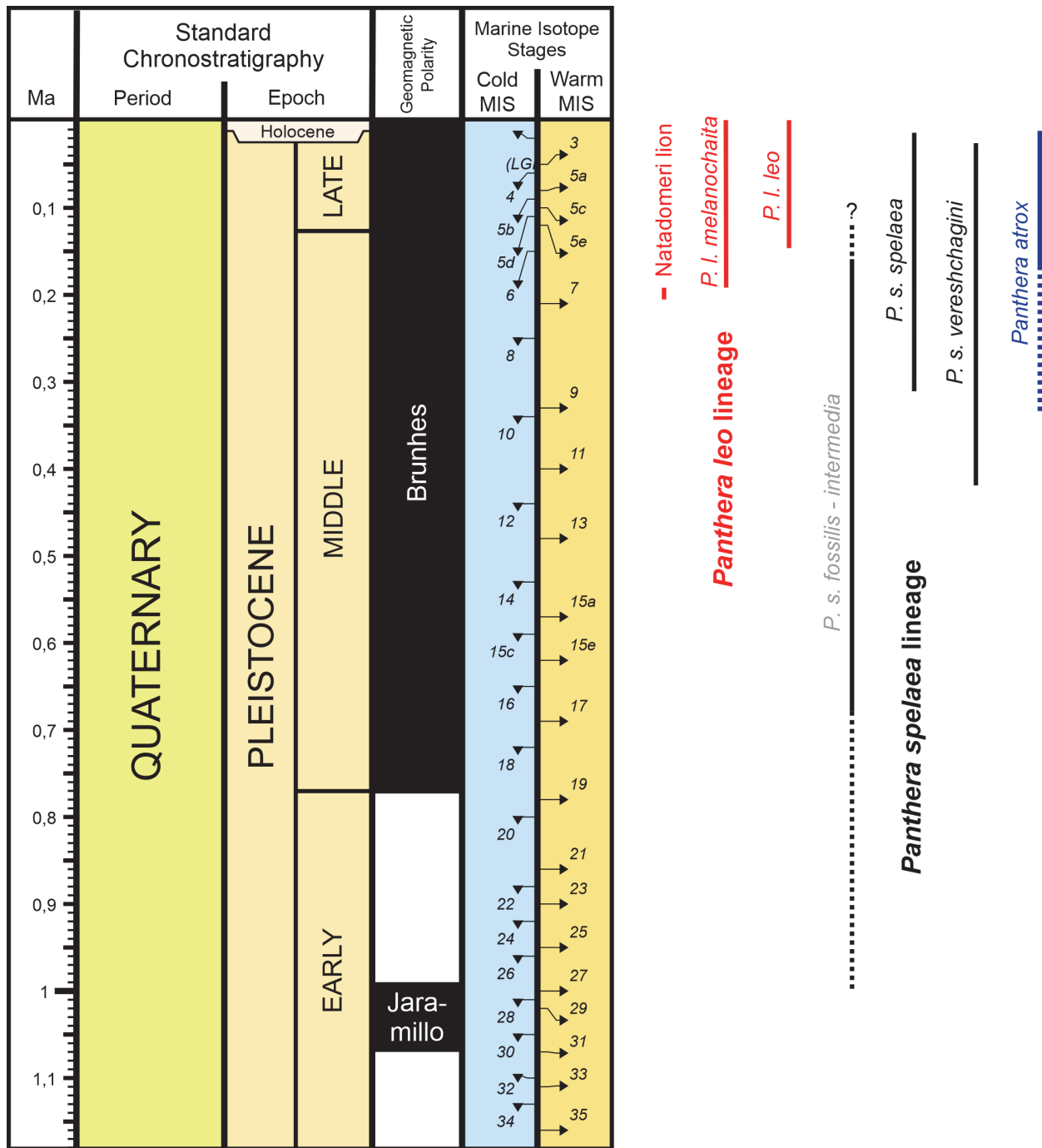


**FIGURE 1.** Chronology of lion lineages based on the data from the fossil record and molecular and paleogenetic researches, referred in the “State of art” section. The grey color in the *Panthera spelaea* lineage suggests questionable evolutionary position of these lion forms. American lions probably represent a separate lineage. The Quaternary chronostratigraphy system is created with the TimeScale Creator software, v. 8.0 (2021).

ably around the middle/late Pleistocene transition (Sabol, 2011). However, Hankó and Korsós (2007) inferred from the cladistic analysis that *P. spelaea* is not a direct descendant of *P. fossilis* but represents a separate, more advanced lineage.

According to molecular and paleogenetic data, the split between extant lion and extinct lion clades could occur approximately 1.85 m.y.a. (Stanton et al., 2020) or 1.89 m.y.a. (Barnett et al., 2016), although younger ages (ca. 500–600 k.y.a.) were

also published (Burger et al., 2004; de Manuel et al., 2020). These latest ages, based only on the molecular estimates or the whole genome data, are too low and do not correspond with the fossil record (Sala, 1990; Lewis et al., 2010).

In *P. leo*, the northern (*P. leo leo*) and southern (*P. leo melanochaita*) lineages are distinguished on the basis of craniometric data (Mazák, 2010), although their morphological diagnoses are so far unknown (Kitchener et al., 2017). Based on the simulation of population history, de Manuel et al. (2020) estimated the divergence between both these *leo* lineages at ca. 70 k.y.a. However, Bertola et al. (2016) put the split of extant lion lineages at 244.8 k.y.a., which better corresponds with the fossil record. In any case, this divergence of the extant lion lineages took place later than in the case of the lineage(-s) of extinct lions, although lion-like felids had existed in Africa for more than 3 m.y.a. (see Sabol, 2011: p. 229–230, and references therein).

The oldest non-African representative of extinct lions is *P. fossilis* occurred in the European fossil record for the first time during MIS 17 (~ 680 k.y.a.) at Pakefield (Lewis et al., 2010) and Kozi Grzbiet (Marciszak et al., 2021), or during MIS 15 (~ 610 k.y.a.) at Isernia la Pineta (Sala, 1990; Hemmer, 2011), respectively. Its first appearance is, however, probably much earlier as evidenced by finds from late early Pleistocene sediments in Western Siberia, correlated with the Jaramillo Subchron (Sotnikova and Foronova, 2014). This lion form persisted at least until MIS 6 period mainly in Europe (Wurm, 1912; Thenius, 1972; Kurtén and Poulianov, 1977; Argant, 1988, 2010; Marciszak et al., 2014, 2019; Sabol, 2014; Argant and Brugal, 2017), from where it is originally mentioned in two chronosubspecies, as *P. spelaea fossilis* (>MIS 17–MIS 10/9) and *P. spelaea intermedia* (~ MIS 10/9–MIS 6) (Argant and Brugal, 2017; Marciszak et al., 2019). These taxa significantly differ, inter alia, in the shape of the nasofrontal cranial profile from late Pleistocene cave lions. The *fossilis*-lineage diverged from other extinct lion lineages certainly more than 1.0 m.y.a., since the first split of cave lion clades is assumed after this period (Stanton et al., 2020). However, this oldest cave lion split (Clade A, 0.97 m.y.a.) should be treated with the caution (Stanton et al., 2020), because it is based only on one site record in Bilibino (Russia) with different radiocarbon data (Kirillova et al., 2015). In addition, the molecular tip dating estimates its age only at 643 k.y.a. (Stanton et al., 2020), which bet-

ter corresponds to the assumed divergence period from the ancestral lineage.

According to Stanton et al. (2020), the better documented split of *speleaea*-lineage (Clades B and C) took place around 578 k.y.a. Clade B can be identified with *P. spelaea vereshchagini* that inhabited Beringia probably in the time span between 419 k.y.a. and 28.0 k.y.a., whereas Clade C contained Eurasian specimens dated between 311 k.y.a. to 12.4 k.y.a. (or 11.2 k.y.a.; see Argant, 2010) and can be identified as *P. spelaea spelaea*. Both subspecies differ significantly in size (Baryshnikov and Boeskorov, 2001) and perhaps also in prey preferences (Guthrie, 1990; Matheus et al., 2003; Bocherens et al., 2011; Diedrich, 2012; Kirillova et al., 2015), although this is conditioned by number of factors. The genetic diversity of cave lions has already been noted by Ersmark et al. (2015) and the division of these extinct felids into at least two groups was also reported in earlier morphometric studies (Hemmer, 1974; Yamaguchi et al., 2004).

American lion, formerly assumed to be a descendant of Asian populations of *Panthera fossilis* (e.g., Sabol, 2011 or Sotnikova and Foronova, 2014) or placed inside the basal diversity of *speleaea*-form with the estimated genetic (reproductive) isolation at around 337 k.y.a. (Barnett et al., 2009), is today rather considered to represent an extinct lineage that diverged from a Beringian population approximately before 165 k.y.a. (Salis et al., 2021). However, these latest paleogenetic data are not supported by morphological analyses (Merriam and Stock, 1932; Simpson, 1941; Kurtén, 1965; Thenius, 1972; Christiansen and Harris, 2009; Benoit, 2010), which suggest that the American lion has retained more primitive characters than the coeval Eurasian cave lion (Sotnikova and Foronova, 2014). In addition, the analyses of mtDNA from American and cave lions are consistent with a degree of reproductive isolation, suggesting some degree of competition between these sister taxa (Barnett et al., 2009). On the other hand, certain dispersal scenarios could also lead to a late divergence date of *P. atrox* with more primitive characters.

The second, subspecies model is based primarily on molecular tip-dating methods (Burger et al., 2004; de Manuel et al., 2020) and supports the subspecies status of all lion forms, belonging to the single species *P. leo* (*P. leo fossilis*, *P. leo spelaea*, *P. leo atrox*). Within the scope of this paper, we follow the species model for the taxonomic determination of analyzed crania of single lion forms.

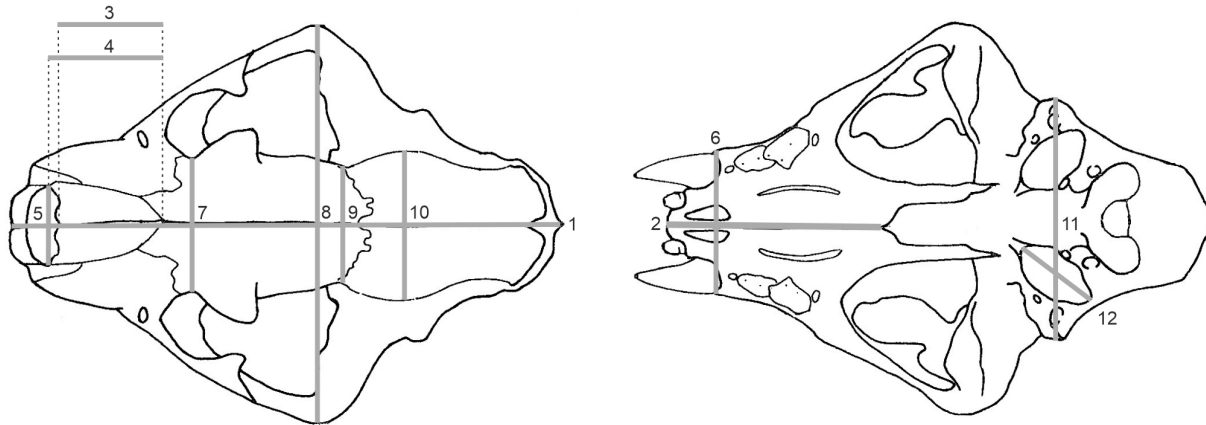


**FIGURE 2.** The 12 linear cranial characters measured on lion crania. 1: greatest cranial length (L, measured as the distance between the prosthion and the acrocranion), 2: palatal length (LP, measured parasagittally as the distance between the prosthion and the staphylion), 3: medial length of nasals (LMN, measured parasagittally as the distance between the naso-frontal suture and the dorsal margin of the external narial opening), 4: lateral length of nasals (LLN, measured as the distance between the naso-frontal suture and the anteriormost tip of the nasal), 5: greatest nasal width (BN, measured at rostral projection of nasals), 6: the snout width (BS, measured at the level of upper canines), 7: interorbital width (IOB, distance between orbits), 8: maximum cranial width across zygomatic arches (BZ), 9: width across postorbital constriction (POC), 10: greatest neurocranial width (BNC, greatest distance between lateral margins of braincase: euryon–euryon), 11: mastoid width (BM, measured across mastoid processes), and 12: greatest diameter of the auditory bullae (LAB). Cranium drawing modified according to Argant (1991).

## MATERIAL AND METHODS

The cranial analyses here were based on original morphometric data collected from paleontological and zoological collections of the Slovak National Museum–Natural History Museum in Bratislava (SNM-PM), Slovak Museum of Nature Protection and Speleology in Liptovský Mikuláš (SMOPaJ), National Museum in Prague (NMP), Moravian Land Museum–Anthropos in Brno (MZMA), and Natural History Museum in Vienna (NHMW) as well as on morphometric data and photographs published in the scientific literature. All analyzed specimens are listed in Appendix 1. The morphometric dataset consisted of 14 main linear cranial measurements, a categorical variable referring to the shape of the cranial profile, and three angle measurements, stratigraphic age, and site altitude of 52 lion-like felid crania (34 adult males and 18 adult females). Among eight crania of the extant lion (from Cameroon, Chad, Senegal, Tanzania, Zambezi, two unknown African sites, and western India) only two specimens belong to animals that originally did not live in the wild (specimens from SNM-PM). The rest of the material is represented by nine crania of *P. atrox* (Ichetucknee, Natural Trap Cave, and Rancho la Brea), two crania of *P. fossilis* (Mauer and Azé I-3), 27 crania of *P. spelaea* (Bottrop, Huttenheim, Perickhöhlen, Siegsdorf, Zoolithenhöhle, Zandobbio, Brno,

Sloup, Srbsko–Chlum, Výpustek 1 and 3, Igrita, Ursilor, Binagady, Desna, Isa, Kondakovka, Mokhokho, Uzhur, and Medvedia Cave in the Western Tatras), and six crania of *P. "intermedia"* (Romain-la-Roche, Vence, Edingen, Niedzwiedzia, San, and Petralona; all originally attributed to "*fossilis-spelaea*" or "*primitive spelaea*" forms). The latter taxon is, according to Argant and Brugal (2017), an intermediate form between steppe and cave lion, and the crania of *P. fossilis* and *P. "intermedia"* are thus assigned to one taxonomic group (*P. fossilis* below). In our analyses, we primarily assessed differences in the size and shape of crania among these four groups (*P. fossilis*, *P. spelaea*, *P. atrox*, and *P. leo*). In some analyses, we also assessed differences between the Western European *P. spelaea* and the Eastern European-Asian *P. spelaea*. As the sexual dimorphism in pantherine cats is relatively high (Mazák, 1980; Mazák, 2004, 2010), we account for the effects of sex by assigning each cranium to male or female on the basis of morphometric data. The assignment of specimen to species is primarily based on non-cranial characters or on other criteria not based on cranial morphology.

The 12 linear cranial characters (Figure 2) are as follows: the greatest cranial length (L), the palatal length (LP), the medial length of nasals (LMN), the lateral length of nasals (LLN), the greatest nasal width (BN), the snout width (BS), the interor-

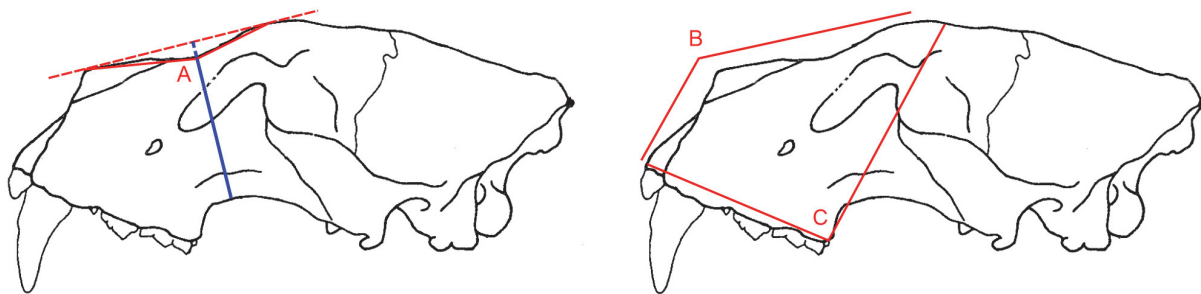


**FIGURE 3.** Profile depths (blue) and angular variables (red) measured on lion crania. Angle A: the cranial profile angle (nasale–frontale angularity), angle B: the angle between narial aperture and nasofrontal profile (premaxillary–nasofrontale angularity), and angle C: the angle between alveolar margin and postorbital process (maxillary–frontale angularity). Cranium drawing modified according to Argant (1991).

bital width (IOB), the width across zygomatic arches (BZ), the postorbital width or constriction (POC), the greatest neurocranial width (BNC), the mastoid width (BM), and the greatest diameter of the auditory bullae (LAB). In addition to these variables, we have measured two profile depths on crania (the profile depth and the profile depth of assumed straight cranial profile) and three angles (the cranial profile angle—angle A, the angle between narial aperture and nasofrontal profile—angle B, the angle between alveolar margin and postorbital process—angle C) to quantify the shape of the nasofrontal region (Figure 3). The profile depth and the cranial profile angle are related to the shape of the profile of the nasofrontal cranial area. In relation to that, three basic types of crania are distinguished (Figure 4)—with straight nasofrontal profile (0), with concave nasofrontal profile (2), and a profile that is intermediate between the two end-member types (1). The measurement methods of lion crania follow Argant (1991) and Christiansen and Harris (2009). The measurements were taken to the nearest 0.1 mm using engineering vernier calipers with 0.3 mm standard deviation, 0.1 mm dispersion, and 4.2% random error. Except for angles, all measured data are given in millimeters (see Appendix 1).

Although the total number of specimens is limited, this cranial morphometric dataset allows us to test whether crania of these apriori-defined species differ with univariate, bivariate, and multivariate methods. Some analyzed crania are, however, incomplete and thus not all cranial characters were measured on these specimens. First, we compared median differences in three angle dimensions among the four groups in univariate analyses (visualized in boxplots and tested with the Wilcoxon rank-sum test). Second, we measured bivariate allometric coefficients between cranial length and

other morphological log-transformed dimensions based on the subsets of crania with the available measurements, using the reduced major axis regressions. Third, to explore multivariate variation in cranial morphology among all specimens, we used the principal coordinate analysis that allows for missing measurements (using Euclidean distances), based on log-transformed dimensions of 14 cranial characters. We use the permutational multivariate analysis of variance (PERMANOVA) to test whether between-group variation on the basis of 14 variables is larger than within-group variation. To summarize, we assessed univariate, bivariate, and multivariate differences in cranial morphology: 1) between *P. fossilis* (incorporating specimens assigned to *P. "intermedia"* to this group) on one hand and *P. spelaea* on the other hand; 2) between nine specimens of *P. spelaea* from Western Europe (Germany and Italy) differ from 18 specimens of *P. spelaea* from Eastern Europe and Asia (Siberia); 3) between *P. atrox* and other groups, and 4) between *P. spelaea* and *P. leo*.

## RESULTS

### Cranial Lengths

The crania of *Panthera* species differ distinctly in size (Miththapala, 1992; Mazák, 2004, 2010) in comparison to crania of lion-like felids, where considerable size overlaps are recorded among species (Turner, 1984; Mazák, 2010; Sabol et al., 2018). Cranial lengths of *P. atrox* and *P. fossilis* tend to be larger than cranial lengths of *P. spelaea*, which are in turn tend to exceed cranial lengths of *P. leo* (Figure 5). However, some differences can be observed when the interorbital width (IOB) and the postorbital constriction (POC) are plotted (Figure 5). The logged POC/IOB ratio of all species observed here generally overlaps with the total

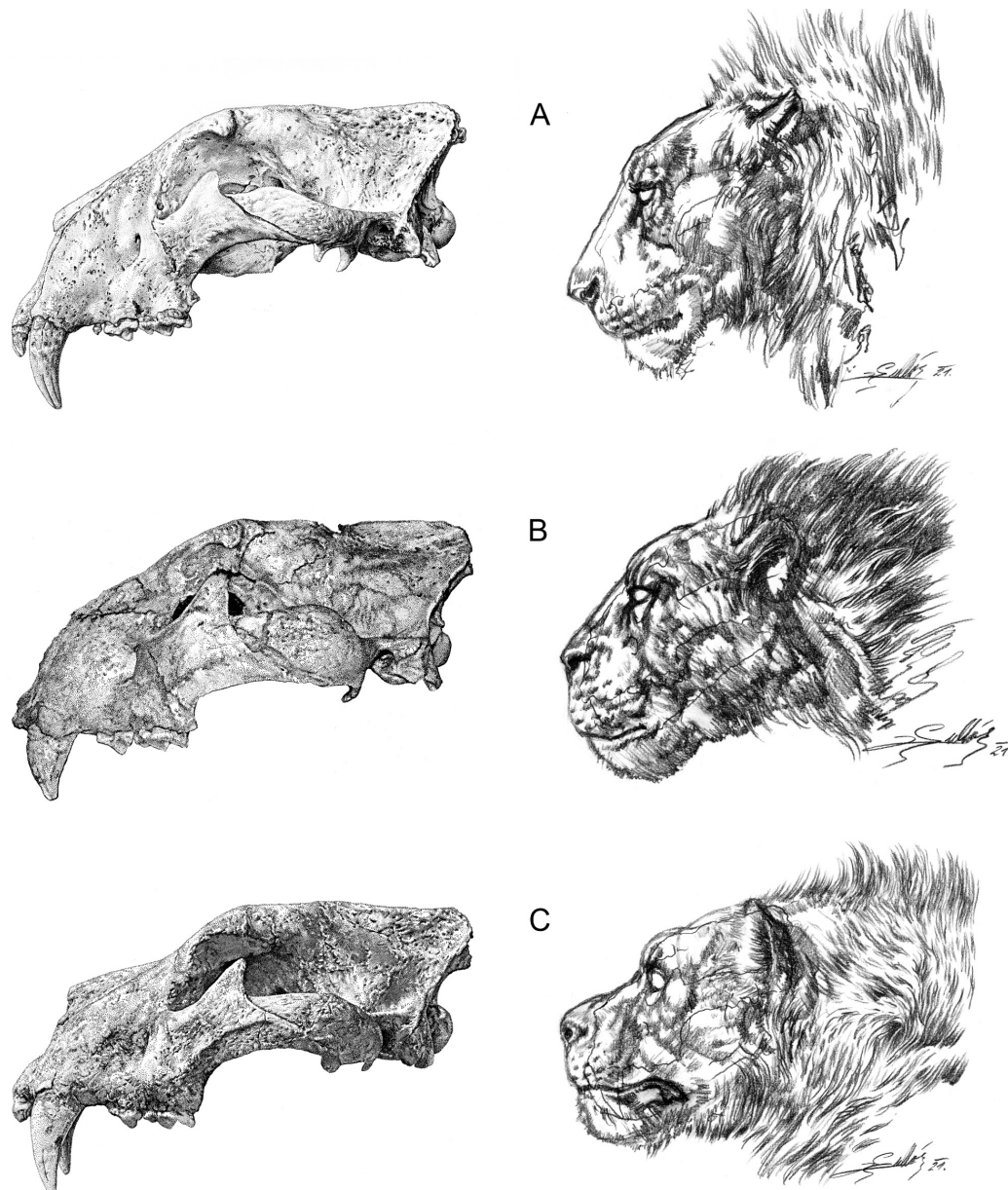


**FIGURE 4.** The types of lion crania distinguished based on cranial profile with the assumed life reconstruction. A: cranium with the straight nasofrontal profile (0)—cranium of *Panthera spelaea* from the Medvedia jaskyňa Cave in the Západné Tatry Mts. in Slovakia (Last Glacial), B: cranium with the intermediate profile between type 0 and type 2 (1)—cranium of *Panthera spelaea* from the Zoolithenhöhle Cave in Germany (Last Glacial), C: cranium with the concave nasofrontal profile (2)—cranium of *Panthera fossilis* from Azé in France (Holsteinian). © J. Gullár, 2011–2021. The crania are not scaled. Author of illustrations is J. Gullár (please, cite it as: J. Gullár in Sabol et al., 2022).

range of variability documented by Mazák (2010) for *P. leo*. However, the median POC/IOB ratio is higher in the Recent *P. leo* (median = -0.02) than in all extinct *Panthera* species (between -0.05 and -0.06; Figure 5). Mazák (2010) also documented that this ratio is sex-dependent, but median per-region POC/IOB ratio is between -0.05 and 0 for

African *P. leo*, whereas it is smaller in Asian *P. leo* and in the Pleistocene *P. spelaea*.

#### Analyses of Profiles and Angles

Other differences are evident in the analysis of the nasofrontal profile. From three defined morphological types, the straight nasofrontal profile (0) prevails in the analyzed lion crania. It was

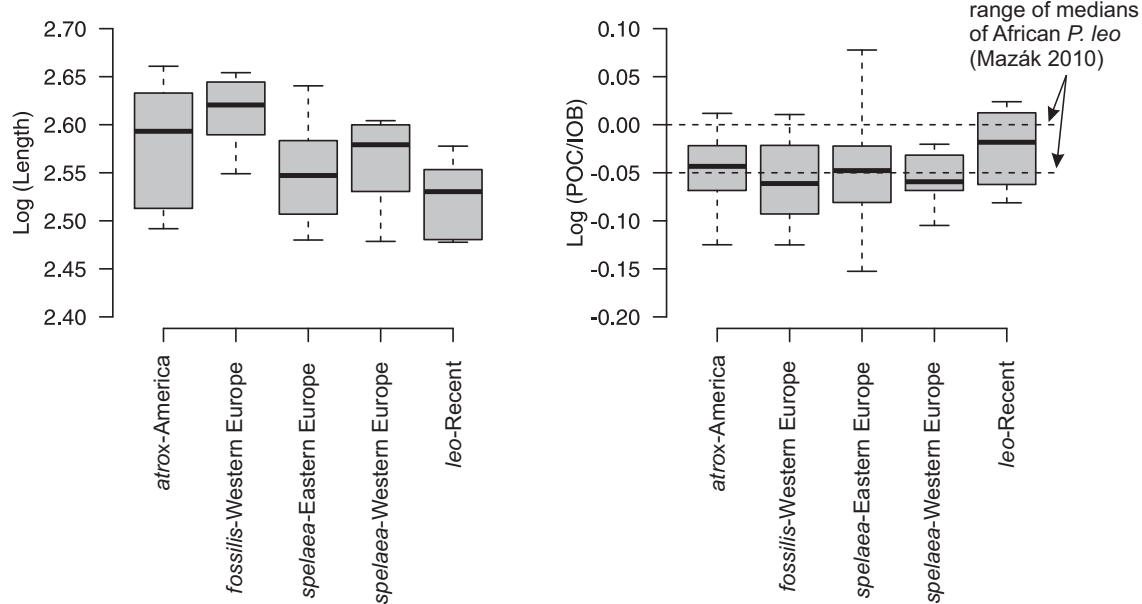


**FIGURE 5.** Boxplots showing differences in cranial length and in the POC/IOB ratio. The horizontal dashed lines approximately span the minima and maxima in *P. leo* from Mazák (2010).

observed predominantly in Last Glacial cave lions from Central and Eastern Europe, but also in Siberian and American lions, as well as in extant *P. leo*. Lions with such nasofrontal profile have also been depicted by Paleolithic artists on the cave walls of Chauvet, La Marche, or Aldène (Figure 6). The concave nasofrontal profile (2) occurs in lion-like felids from the mid-middle Pleistocene (Holsteinian) to the early late Pleistocene (Eemian), mainly of Western Europe and Poland (Niedźwiedzia and San), but sporadically also in crania from the Last Glacial of Moravia (Sloup Cave) or even from Siberia (Kondakovka). This type of profile was probably present also in lion cranium from Mauer (*P. fossilis*) and is clearly visible on some manifestations of the Paleolithic art, such as lion head sculpture from Kostenki (Figure 6). A “link” between above mentioned cranial profiles (1) is rarely observed in lion crania from Edingen, Petralona, Zoolithen, and also in extant lions (SNM-PM C 1521 and SNM-PM 1701). Based on the figured giant lion cranium from Kenyan site of Natodomeri (Manthi et al., 2017, figure 3), it seems that this individual could also belong to this group.

Boxplots in Figure 7 show that cranial variables related to the shape of their nasofrontal profile discriminate between crania assigned to *P. fossilis* and *P. "intermedia"* on one hand and those assigned to *P. spelaea* on the other hand. The profile angle (angle A) is significantly less concave (Wilcoxon test,  $p<0.001$ ) and the premaxillary-

nasofrontal angularity (angle B) is significantly larger, i.e., less sharp (Wilcoxon test,  $p<0.001$ ) in *P. spelaea* (median profile angle = 174–175°, median of angle B = 141–144°) than in *P. fossilis* (median profile angle = 164°, median of angle B = 138°). The profile angle is also less concave in *P. atrox* (median profile angle = 177°, median of angle B = 143°) than in *P. fossilis*. The median of angle B is also significantly higher in *P. leo* (149°) relative to *P. spelaea* (Wilcoxon test,  $p=0.02$ ) and in other species. Therefore, these groups of lions can be discriminated on the basis of the profile of the nasofrontal region. The two geographic subgroups of *P. spelaea* do not differ in the three angle characters (Wilcoxon test,  $p<0.001$ ).

#### Bivariate Allometric Coefficients

Bivariate relationships between the cranial length and other morphological variables document some consistent between-group differences in allometric coefficients (Figures 8–9). First, although 95% confidence intervals tend to be broad, these coefficients demonstrate more positive allometry for mastoid width, snout width, medial nasal length, and lateral nasal length in *P. fossilis* relative to other three species. Second, the postorbital width (POC) increases slowly with increasing cranial length (negative allometry) in *P. leo* and in *P. atrox* whereas it increases at higher rate in *P. spelaea* and *P. fossilis*. Third, zygomatic width, snout width, and medial nasal length

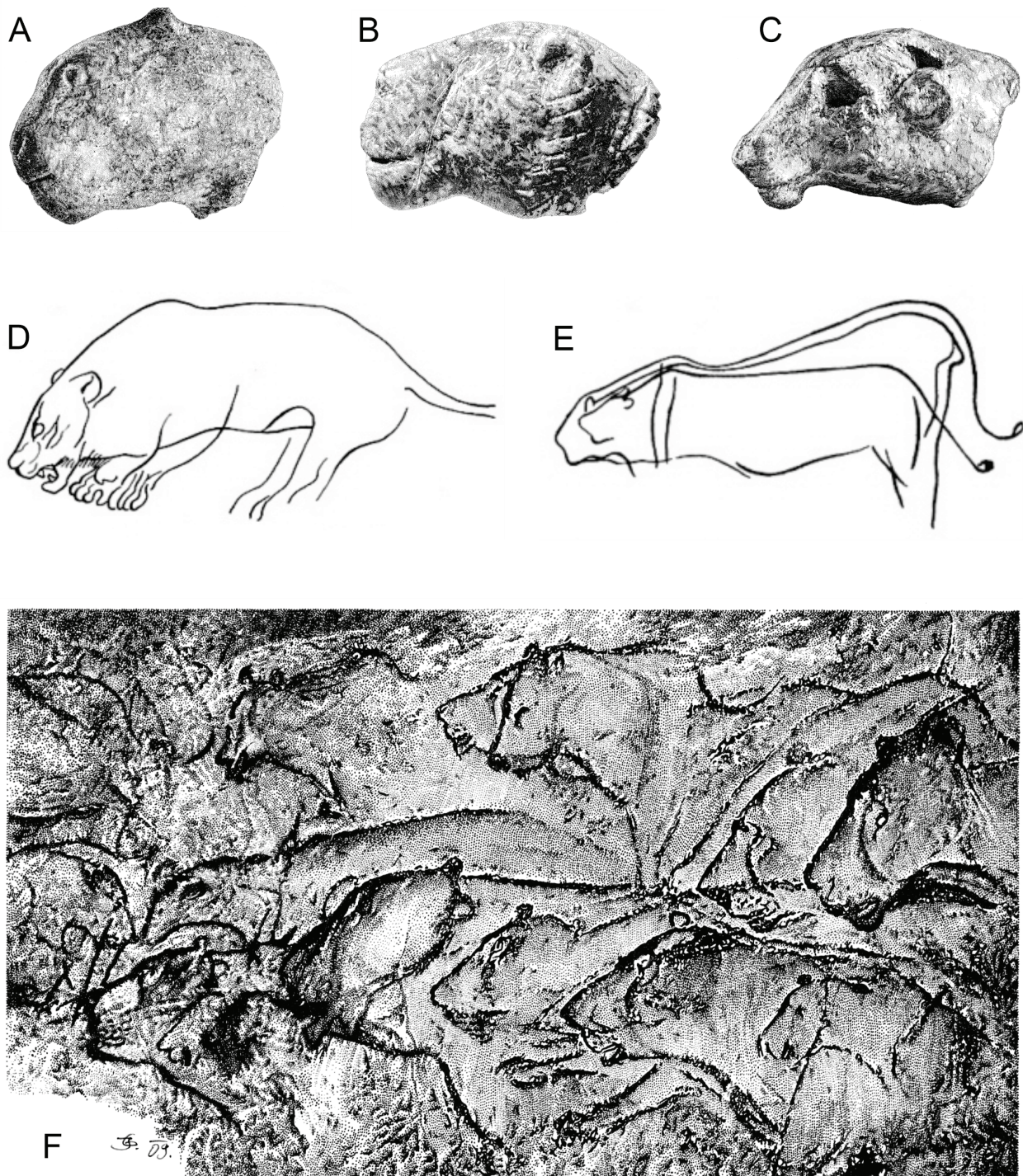


**FIGURE 6.** Different types of lion heads in Paleolithic art, maybe indicating the cranial profile type 2 (A), probably the cranial profile type 1 (B), and the cranial profile type 0 (C-F). A: a lion head sculpture from Kostenki near Voronezh, Russia (ca. 23 ka BP, redrawn from Efimenko 1958); B: a lion head sculpture from Vogelherd, Germany (ca. 38-33 ka BP, redrawn from Koenigswald and Schmitt 1987); C: a lion head sculpture from Dolní Věstonice, Moravia–Czech Republic (ca. 27-29 ka BP, redrawn from Jelínek 1972); D: a cave lion depicted in La Marche, France (Magdalenian); E: cave lion pair depicted in Chauvet, France (< 26 ka BP); F: cave lions depicted in Chauvet, France (< 26 ka BP, redrawn from Clottes 2001). © J. Gullár, 2009-2014 (A–C, F) and the archive of M. Sabol (D and E). Author of illustrations A–C and F is J. Gullár (please, cite it as: J. Gullár in Sabol et al., 2022); D and E are from the archive of M. Sabol.

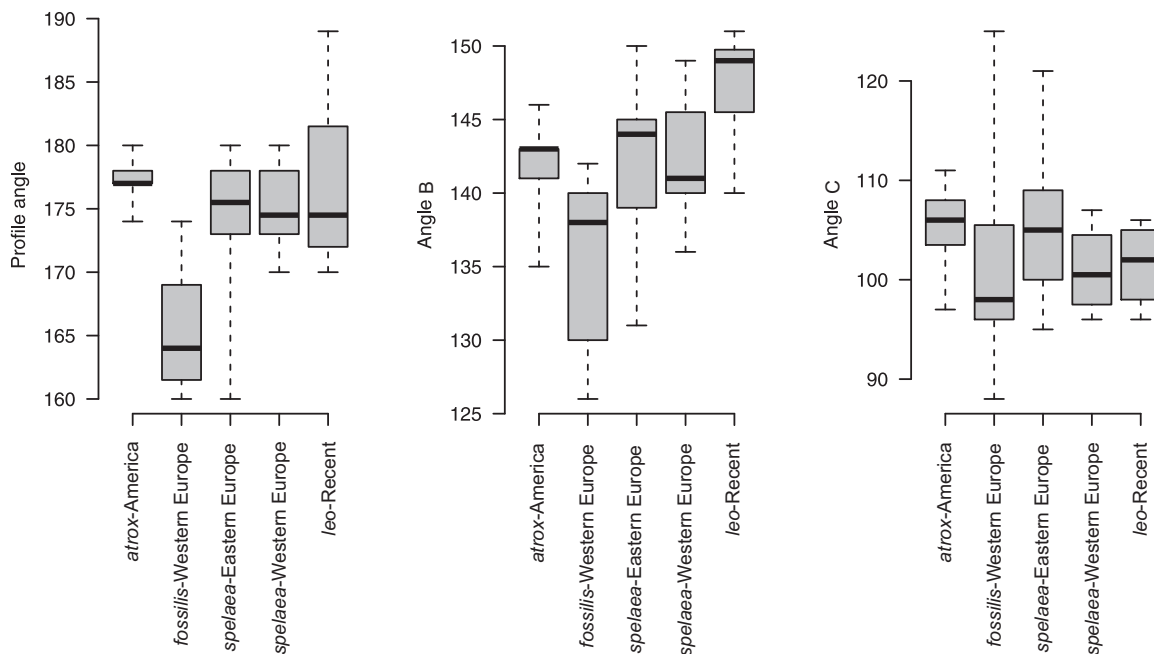


**FIGURE 7.** Boxplots (median values and the 25<sup>th</sup> and 75<sup>th</sup> quantiles, with whiskers showing extreme values) showing that the profile angle and the angle B discriminate between *P. fossilis* on one hand and other groups of taxa on the other hand. *P. leo* has higher median angle B than other extinct species of the genus *Panthera*.

increases at slower rate relative to the cranial length in *P. atrox* (negative allometry) relative to other species where these traits show positive allometry (Figure 9). It can be seen in Figure 8G that the palatal length shows an isometric relation relative to overall size in all species, but the difference in intercepts between *P. atrox* and the other groups effectively contributes to the second PCO axis that separates the American lion from other species. The postorbital constriction width shows positive allometry in *P. fossilis* and *P. spelaea*, but negative allometry in *P. leo* and *P. atrox* (Figure 8I).

### Multivariate Analyses

The first two axes of principal coordinate analysis (PCO) explain 92% of among-specimen variation in cranial morphology (Figure 10A). First, multivariate analysis of variance shows that on the basis of 14 cranial characters, *P. atrox* is clearly segregated from other *Panthera* species along the PCO axis 2 (PERMANOVA  $F=5.05$ ,  $p=0.01$ ). Second, crania of *P. fossilis* (including *P. "intermedia"*) differ weakly from *P. spelaea* ones, with borderline significance (PERMANOVA  $F=3.5$ ,  $p=0.04$ ), being primarily separated along the PCO axis 2. Third, *P. spelaea* crania are characterized by high variability that overlaps to some degree with *P. leo* and with *P. fossilis*. However, despite this overlap, the distance between multivariate means of *P. spelaea*

crania from Eastern Europe and Western Europe is higher than within-group distances between the means and crania of constituent individuals (PERMANOVA,  $F=6.02$ ,  $p=0.004$ ), and are partly separated along the PCO axis 1. However, *P. fossilis* and *P. "intermedia"* do not differ from the Western European assemblage of *P. spelaea* alone, and the overall difference between *P. spelaea* (across its whole geographic range) and *P. fossilis* is driven by the Eastern European assemblage of *P. spelaea*. In turn, pooling the crania of *P. spelaea* from western regions with *P. fossilis* and *P. "intermedia"* into one group forms a set that significantly differs from crania of *P. spelaea* from Eastern Europe and Asia (PERMANOVA  $F=5.1$ ,  $p=0.003$ ). Morphological differences between geographic variants of *P. spelaea* and among *P. spelaea* and other forms remain in the PCO analysis when *P. atrox* is excluded (Figure 10B). Figure 11 shows that all variables strongly correlate with the PCO axis 1 (with weaker correlations related to braincase width and auditory bulla), similarly as in the exhaustive analysis based on all species, and the nasale width, palatal length, auditory bulla, and the full profile depth correlate with the PCO axis 2. The morphological separation among *P. fossilis* and *P. spelaea* still occurs along the PCO axis 1, with a marked overlap between the Western forms of *P. spelaea* and *P. fossilis*. However, *P. fossilis* is also slightly offset along the

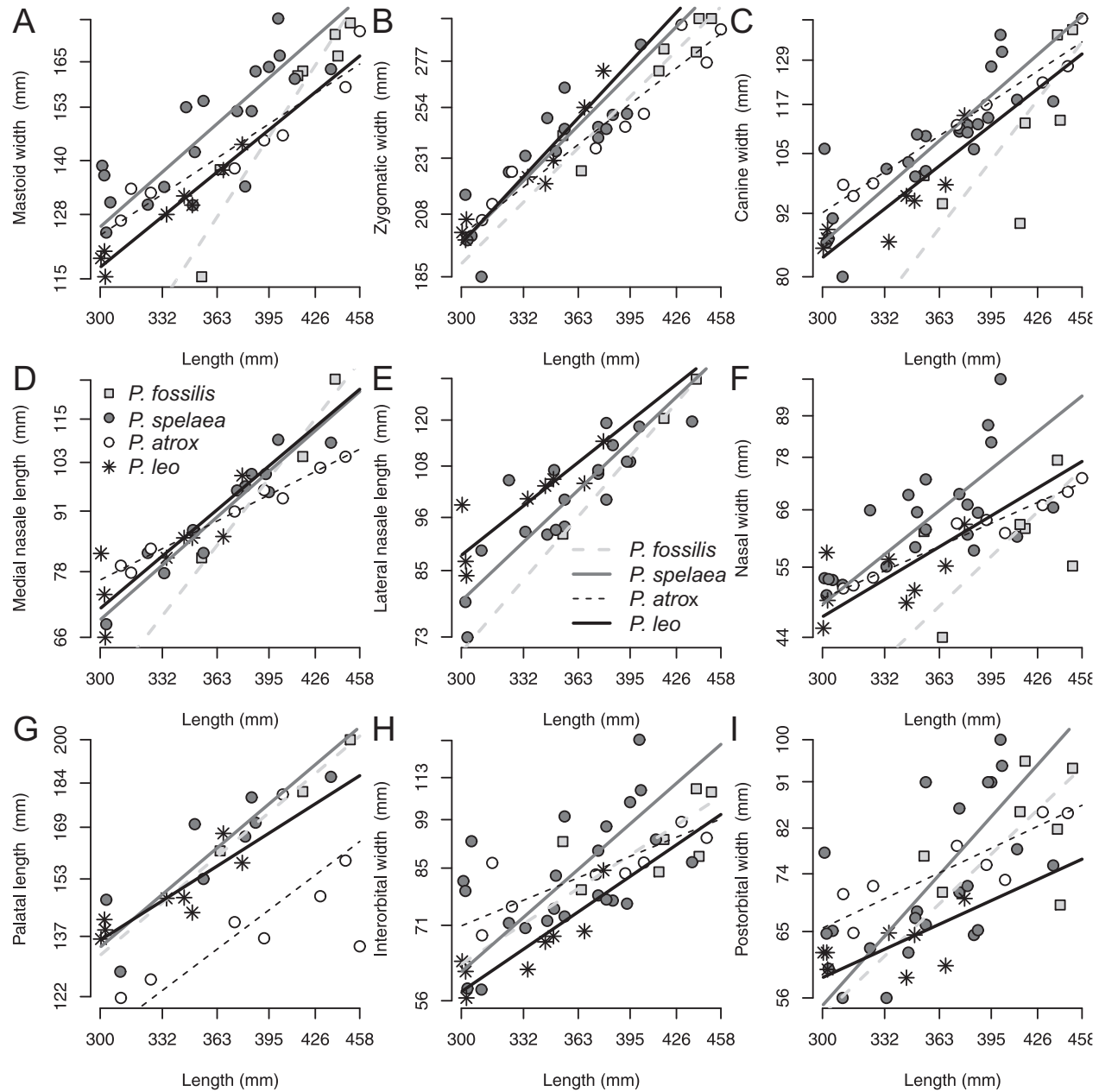


**FIGURE 8.** Bivariate relationships between the cranial length and nine morphological variables. The lines represent slopes of the relationship between the log-transformed cranial length and nine variables fitted by reduced major axis regression separately for *P. fossilis*, *P. spelaea*, and *P. leo*. Axes are logged.

PCO axis 2, indicating that a shift in morphospace is unrelated to size-related shift in morphology along the PCO axis 1.

We note that the effects of sexual differences and altitudinal effects are small and insignificant, although the detection of such effects is limited by the small sample size (i.e., small number of crania).

## DISCUSSION

### Relationships Between Extinct and Extant Lions

The morphological differences in the dentition and skulls between extinct (Hemmer, 1974; Baryshnikov and Boeskorov, 2001; Yamaguchi et al., 2004; Sotnikova and Nikolskiy, 2006; Barycka, 2008; Christiansen and Harris, 2009; Benoit, 2010; Marciszak et al., 2014, 2019) and extant lions

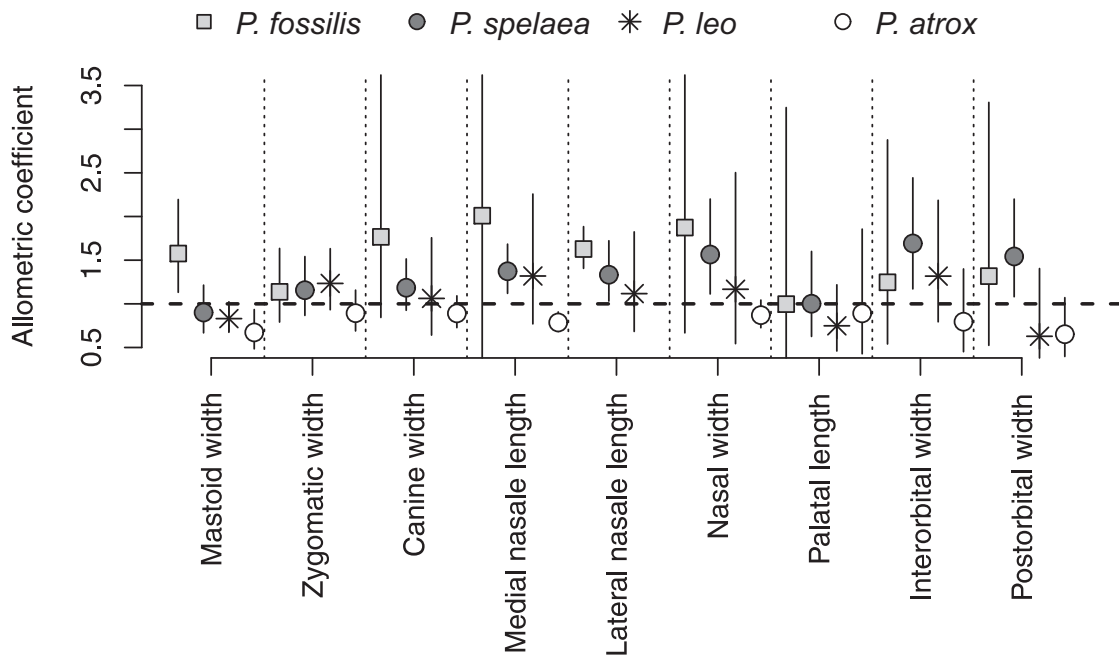


**FIGURE 9.** The summary of mean allometric coefficients (slopes of the relationship between the log-transformed cranial length and nine variables fitted by reduced major axis regression) with 95% bootstrapped confidence intervals. They show more positive allometry for mastoid width, canine width, medial nasale length, and lateral nasal length in *P. fossilis* relative to other three species (although 95% confidence intervals are broad). The postorbital width shows negative allometry in *P. leo* whereas it shows positive allometry in *P. spelaea* and *P. fossilis*. The missing values in *P. atrox* did not allow to measure its allometric coefficients for lateral nasal length.

(Mazák, 2010) in former analyses indicated a certain variability, what was also reflected in taxonomic studies still before the more demonstrable results of molecular and paleogenetic analyses. One of the most conspicuous different features in the cranial morphology is a shape of the cranial profile in the nasofrontal region, known also from the Paleolithic art. Our analyses confirm the existence of differences in cranial morphology between extinct and extant lions. These analyses also show some geographic differences between the Pleistocene forms themselves, although the overall within-group variability exceeds differences among groups (e.g., between Western European *P. spelaea* and *P. fossilis*), and the cranial morphology rather supports the chronospecies model.

The crania of *P. leo* are generally smaller, showing the higher median POC/IOB ratio and the higher median of angle B compared to crania of extinct lions. On the other hand, Hemmer (1974) mentioned certain similarities of modern North African–Asian lions with the middle Pleistocene lions in cranial morphology. But the “*fossilis–intermedia*” lions are clearly different from other lions in the distinct concave nasofrontal profile and demonstrate also more positive allometry for the mastoid width, snout width, medial nasale length, and lateral

nasale length. When results of multivariate analyses are considered, their crania show some resemblance to those of Western European cave lions, which are separated from crania of cave lions from the Eastern European–Asian region. However, both these geographical subgroups of cave lions do not differ in their angle characters. The division of European cave lions into at least two groups (west and east ones) based on cranial morphology was first pointed out by Hemmer (1974), and later also by Yamaguchi et al. (2004) or by Barycka (2008). This variability observed was considered either as a consequence of the invasion of Siberian lions (Hemmer, 1974) or as a result of the penetration of modern lions from SW Asia already during the Pleistocene (Yamaguchi et al., 2004).

#### Relationships Between *P. atrox* and Other Lions

Unlike to above mentioned lion taxa, the American lions form a separate, clearly different group in our multivariate analysis. This separation supports the results of some previous morphological observations (Merriam and Stock, 1932; Thenius, 1972; Martin and Gilbert, 1978; Baryshnikov and Boeskorov, 2001; Christiansen and Harris, 2009; Benoit, 2010; Sakamoto and Ruta, 2012).

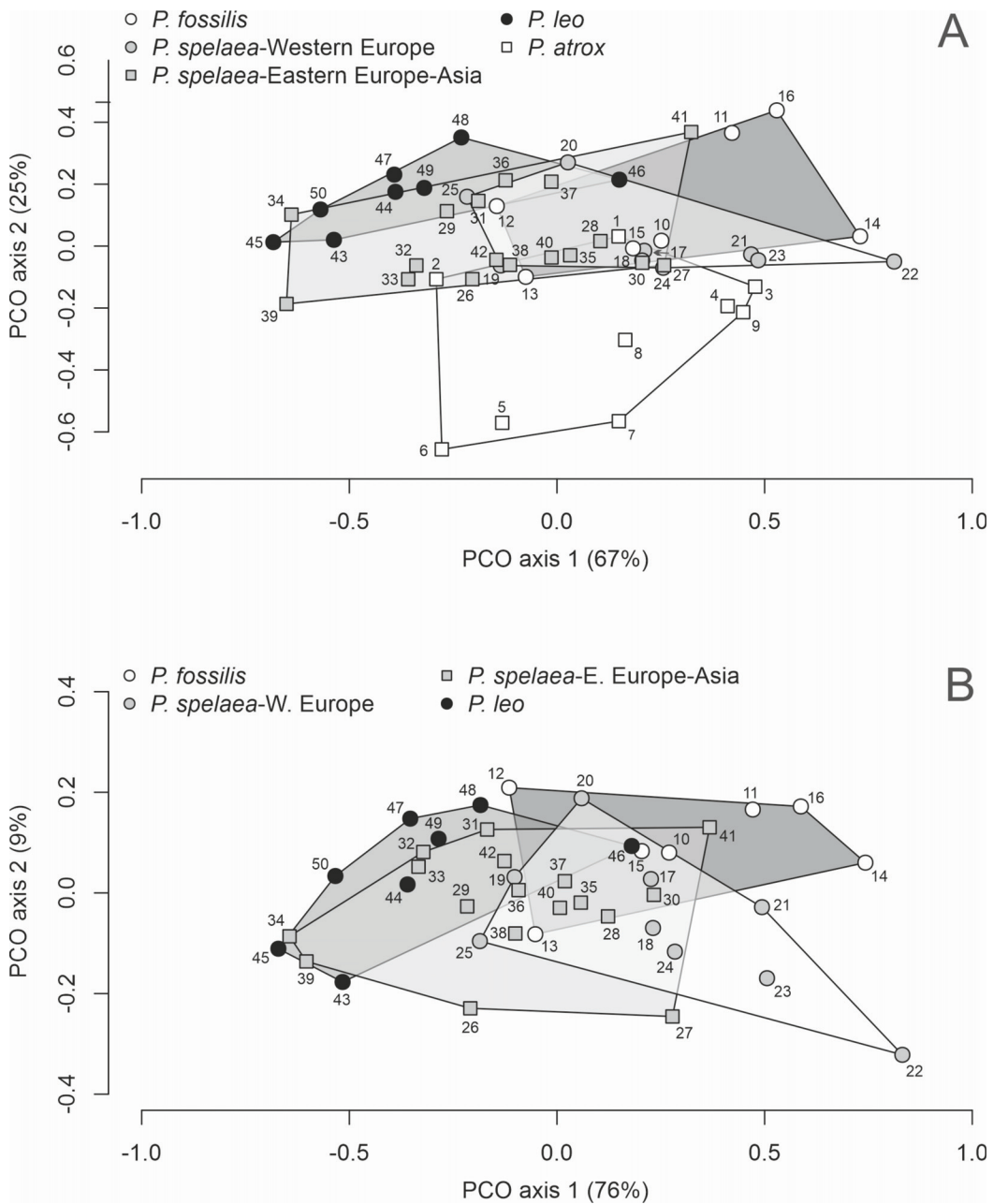


**FIGURE 10.** A: Principal coordinate analyses based on 14 log-transformed morphometric variables. The first axis is parallel with an overall increase in cranial length. Across its whole range, *P. spelaea* differs from *P. fossilis*, and *P. fossilis* is clearly distinct from *P. leo*. However, *P. spelaea* from the Western Europe alone does not differ from *P. fossilis*. B: Principal coordinate analyses based on 14 log-transformed morphometric variables, excluding *P. atrox*. This analysis shows that *P. spelaea* from the Western Europe and the Eastern Europe–Asia do not fully overlap in morphospace. The first PCO axis in both analyses correlates strongly positively with all variables and thus reflects the size axis. Specimen numbers: *P. atrox* (North America): 1–Ichetucknee, 2–Natural Trap Cave, 3–9–Rancho la Brea; *P. fossilis*: 10–Mauer (Germany), 11–Azé I-3 (France); *P. intermedia*: 12–Romain-la-Roche (France), 13–Vence (France), 14–Edingen (Germany), 15–Niedzwiedzia Cave (Poland), 16–San (Poland); *P. spelaea*: 17–Bottrop (Germany), 18–Huttenheim (Germany), 19–Perickhöhlen (Germany), 20–Siegsdorf (Germany), 21–Zoolithenhöhle (holotype; Germany), 22–24–Zoolithenhöhle (Germany), 25–Zandobbio (Italy), 26–Brno (Czech R.), 27–Sloup (Vienna specimen; Czech R.), 28–Sloup (OK 130570, Czech R.), 29–Srbsko–Chlum Komín Cave (Czech R.), 30–Výpustek 1 (Czech R.), 31–Výpustek 3 (Czech R.), 32–Igrita (Croatia), 33–Ursilor (Romania), 34–Binagady (Caucasus, Georgia), 35–Desna (Russia), 36–37–Isa River (South Ural, Russia), 38–Kondakovka (Russia), 39–Mokhokho (Russia), 40–Uzhur (Central Siberia), 41–42–Medvedia Cave (Slovakia); *P. leo* (Africa and India): 43–50.

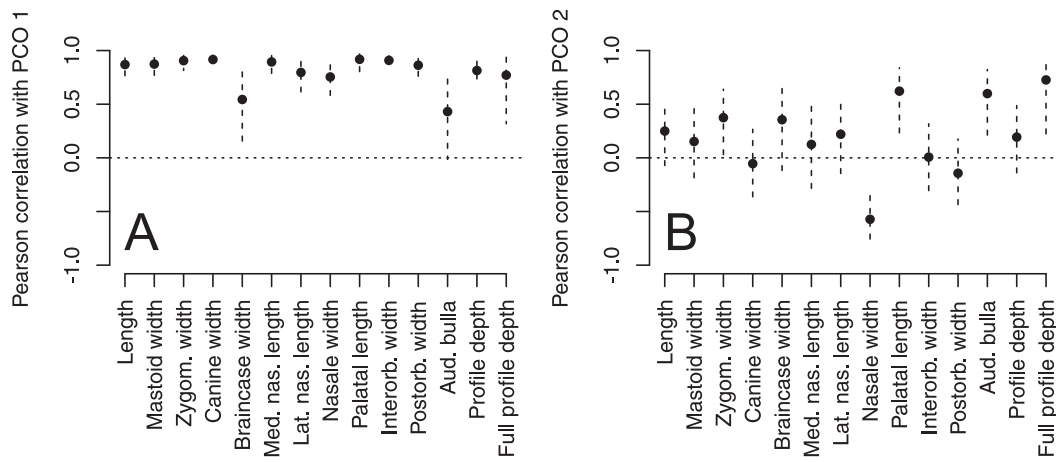


**FIGURE 11.** A–B: Pearson correlations between the 14 variables and the two PCO axes based on *P. leo*, *P. spelaea*, and *P. fossilis* (thus excluding *P. atrox*, corresponding to Figure 10B).

On the other hand, their crania are also characterized by the straight nasofrontal profile, which is predominantly present in most crania of cave and modern lions.

#### Relationships Between *P. spelaea* and *P. fossilis*—Chronospecies Model

Based on the differences in the cranial morphology observed among individual lion forms, these could constitute separate taxonomic units, as assumed by the species model. However, the originally estimated age of the split of extinct lion lineage(s) from the extant one (Burger et al., 2004) based on molecular tip-dating (ca. 0.6 m.y.a.) did not support their taxonomic status as separate species since the entire extinct lion clade(-s) was considered too young (at least according to the criteria of Kitchener et al., 2017). On the other hand, if dating using the fossil record and some recent molecular data (Stanton et al., 2020) are correct, this split between extant and extinct lion lineages must have already occurred during the early Pleistocene (ca 1.8–1.9 m.y.a.). In this case, extinct lions would be acceptable as a Holarctic clade distinct from the *P. leo* clade, forming at least one separate species (*P. spelaea*) with some subspecies. Its division into several separate species is also not excluded, but their taxonomic position may not be stable in terms of the value of observed morphological characters, which may be related to various factors influenced by local climate and environmental conditions. A similar situation can also be observed in the study of cave hyenas, where it is still discussed whether European and Asian populations are different species, even though they were separated for at least 2.0 million years ago (Westbury et al., 2020).

However, multivariate analyses show, first, that the major axis of variation among specimens of *P. spelaea* and *P. fossilis*—*P. “intermedia”* occurs along the first PCO axis, but this axis also correlates with the size of all variables (with the exception of palatal length). As in many other similar morphometric analyses, this axis thus largely captures size variability. Therefore, morphological differences between the western and eastern forms of *P. spelaea* as well as between the cave lions and *P. fossilis*—*P. “intermedia”* can be largely accounted for by size variation. Second, high variability of *P. spelaea* is probably accentuated by long temporal coverage of specimens of this species (middle–late Pleistocene, up to the Last Glacial Maximum) relative to the snapshot nature of *P. leo* specimens collected just in the twentieth century. Longer temporal span of morphometric variability assessed over long temporal duration (covered specimens of *P. fossilis* and *P. spelaea*) can be coupled with the temporally–shifting adaptive landscape, leading to presence of transient traits related to temporally–unique climatic conditions or to the development of transient geographic barriers.

In fact, the species defined in the fossil record often represent only the chronospecies of a continually–evolving biospecies. *P. fossilis* and *P. spelaea* can represent such an example of a chronospecies (as also inferred for hyenas; Rohland et al., 2005). Although these lions are considered to be a separate species based on their morphological characters and, of course, stratigraphic position, our analyses indicate high overlap between these two temporally–separated forms, suggesting that they rather grade into each other.

The American lion can retain a separate species status, because it distinctly differs from other lions in morphology and paleobiogeographical distribution. Its separate position in our analyses can result from its rapid divergence after dispersal to the southern part of North America. From this point of view, a higher number of well-preserved and stratified cranial material, analytically also integrated with non-cranial data, will be needed to future confirm the subspecies model in lions.

Multivariate analysis of all forms that potentially belong to one chronospecies indicates that one source of variation relates to geographic partitioning of populations. On one hand, the morphometric patterns that show the gradation between Eastern and Western European *P. spelaea* and their relation to *P. fossilis* can suggest that the West-European *P. spelaea* is more related to *P. fossilis* and *P. "intermedia"* lineage and the East-European *P. spelaea* is related to immigrants from Siberia. On the other hand, the similarity between the West-European specimens (as immigrants from the East) and specimens of *P. fossilis*–“*intermedia*” can reflect a functional convergence to similar environmental and climatic conditions prevailing in Western Europe. More complex scenarios due to secondary mixing or hybridization among populations of different (sub-)species are also possible.

One of the last unresolved questions, although beyond the scope of this paper, is related to the causes of the transition from concave to straight nasofrontal profile during the evolution of lions. The influence of sexual differences and altitudinal effects in this process was negligible, and the formerly assumed influence of the individual age on the cranial profile shape (Schütt and Hemmer, 1978) was also shown as insignificant. A similar transition is observed between the crania of brown bear (*Ursus arctos*), with a more concave nasofrontal profile, and polar bear (*Ursus maritimus*), with a straighter nasofrontal profile. This transition is probably caused by adaptation to life in colder climatic conditions and/or by different dietary requirements. Did similar processes also play a role in the “straightening” of the nasofrontal profile on lion crania? Although the role of cold climate and diet preferences cannot be completely ruled out, other factors have probably played a role here, as straight nasofrontal profiles also occur in modern lions inhabiting subtropical to tropical climate zones. It seems that this transition could be related to the adaptation to hunting of large, meta-

bolically valuable prey (Carbone et al., 1999). According to Sakamoto and Ruta (2012), however, the shape of cranium may not have been a result of direct selection forces, and its evolution was rather a result of selection based on the influence of latent factors such as function, ecology/environment, or development.

## CONCLUSION

The craniometric dissimilarities documented in our study visualize certain variations among extinct and extant lions, which can relate to phenotypic variances or can also indicate a more distinct differentiation among separate lion forms what can relate to a different range of their temporal and spatial distribution. The results of our analyses show that, with the exception of American lion, the overall differences between *fossilis* and *spelaea* groups (1) are rather minor and reflect differences in size and allometric consequences, but (2) are also affected by high size and shape variation that is geographically structured, with the partial difference between the Western and Eastern European forms of *P. spelaea* and with a similarity between the Western European *P. spelaea* and *P. fossilis*. These lions can, therefore, be considered as chronospecies within one common clade (*P. spelaea*). However, this chronospecies model should be supported with further research, as the similarity in some cranial characters between middle Pleistocene steppe lions (*fossilis*–“*intermedia*”) and Western European cave lions from the late Pleistocene may not only indicate phylogenetic affinity but may also reflect a functional convergence based on similar environmental and climatic conditions prevailing in Western Europe. The cranial variability observed between Western European and Eastern European–Asian cave lions could be related to various migration events. The American lion clearly differs from other lion forms and could be considered a separate taxon (*P. atrox*). The observed different characters in the cranial morphology of the extant lions also support their independent species status (*P. leo*) with respect to extinct lion forms. The future research should include not only the higher geographic coverage of the cranial material but also non-cranial material, and a better understanding of lion evolution can only be obtained by integrating diverse analytical procedures. In this context, the trend towards the straightening of the nasofrontal profile of lion crania during the Pleistocene can also be resolved.

## ACKNOWLEDGMENTS

The research for this paper was carried out with financial support from the Slovak Research and Development Agency (project APVV-20-0079 [M.S.]) and from the Slovak Scientific Grant Agency (project VEGA 0169/19 [A.T.]). The authors

also gratefully acknowledge the helpful comments and suggestions of anonymous reviewers for improvement of the manuscript. Their gratitude goes also to Editor M. Stewart for handling the manuscript.

---

## REFERENCES

- Argant, A. 1988. Etude de l'exemplaire de *Panthera spelaea* (Goldfuss, 1810) (Mammalia, Carnivora, Felidae) du gisement Pleistocene moyen récent de la grotte d'Aze (Saône et Loire). Revue de Paléobiologie, 7:449-466.
- Argant, A. 1991. Carnivores quaternaires de Bourgogne. Documents des Laboratoires de Géologie, 115:3-304.
- Argant, A. 2010. Carnivores (Canidae, Felidae et Ursidae) de Romain-la-Roche (Doubs, France). Revue de Paléobiologie, 29:495-601.
- Argant, A. and Brugal, J.-P. 2017. The cave lion *Panthera (Leo) spelaea* and its evolution: *Panthera spelaea intermedia* nov. subspecies. Acta Zoologica Cracoviensia, 60(2):59-104. [https://doi.org/10.3409/azc.60\\_2.59](https://doi.org/10.3409/azc.60_2.59)
- Barnett, R., Shapiro, B., Barnes, I., Ho, S.Y.W., Burger, J., Yamaguchi, N., Higham, T.F.G., Wheeler, H.T., Rosendahl, W., Sher, A.V., Sotnikova, M., Kuznetsova, T., Baryshnikov, G.F., Martin, L.D., Harington, C.R., Burns, J.A., and Cooper, A. 2009. Phylogeography of lions (*Panthera leo* ssp.) reveals three distinct taxa and a late Pleistocene reduction in genetic diversity. Molecular Ecology, 18:1668-1677. <https://doi.org/10.1111/j.1365-294X.2009.04134.x>
- Barnett, R., Yamaguchi, N., Shapiro, B., Ho, S.Y.W., Barnes, I., Sabin, R., Werdelin, L., Cuisin, J., and Larson, G. 2014. Revealing the maternal demographic history of *Panthera leo* using ancient DNA and a spatially explicit genealogical analysis. BMC Evolutionary Biology, 14(70):1-11. <https://doi.org/10.1186/1471-2148-14-70>
- Barnett, R., Zepeda Mendoza, M.L., Rodrigues Soares, A.E., Ho, S.Y.W., Zazula, G., Yamaguchi, Y., Shapiro, B., Kirillova, I.V., Larson, G., and Gilbert, M.T.P. 2016. Mitogenomics of the extinct cave lion, *Panthera spelaea* (Goldfuss, 1810), resolve its position within the *Panthera* cats. Open Quaternary, 2(4):1-11. <https://doi.org/10.5334/oq.24>
- Barycka, E. 2008. Middle and late Pleistocene Felidae and Hyaenidae of Poland. Fauna Poloniae – Fauna Polski 2ns. Museum and Institute of Zoology Polish Academy of Science, Warszawa.
- Baryshnikov, G. and Boeskorov, G. 2001. The Pleistocene cave lion, *Panthera spelaea* (Carnivora, Felidae) from Yakutia, Russia. Cranium, 18(1):7-23.
- Baryshnikov, G.F. and Tsoukala, E. 2010. New analysis of the Pleistocene carnivore from Petralona Cave (Macedonia, Greece) based on the collection of the Thessaloniki Aristotle University. Geobios, 43:389-402. <https://doi.org/10.1016/j.geobios.2010.01.003>
- Benoit, M.H. 2010. What's the difference? A multiphasic allometric analysis of fossil and living lions, p. 165-188. In Goswami, A. and Friscia, A. (eds.), Carnivoran Evolution. New views on phylogeny, form and function. Cambridge Studies in Morphology and Molecules. New paradigms in Evolutionary Biology. Cambridge University Press, Cambridge.
- Bertola, L.D., Jongbloed, H., Van Der Gaag, K.J., De Knijff, P., Yamaguchi, N., Hooghiemstra, H., Bauer, H., Henschel, P., White, P.A., Driscoll, C.A., Tende, T., Ottosson, U., Saidu, Y., Vrieling, K., and De longh, H.H. 2016. Phylogeographic patterns in Africa and High Resolution delineation of genetic clades in the Lion (*Panthera leo*). Scientific Reports, 6(1):30807. <https://doi.org/10.1038/srep30807>
- Bocherens, H., Drucker, D.G., Bonjean, D., Bridault, A., Conard, N.J., Cupillard, C., Germonpré, M., Höneisen, M., Müntzel, S.C., Napierala, H., Patou-Mathis, M., Stephan, E., Uerpmann, H.P., and Ziegler, R. 2011. Isotopic evidence for dietary ecology of cave lion (*Panthera spelaea*) in North-Western Europe: Prey choice, competition and implications for extinction. Quaternary International, 245:249-261. <https://doi.org/10.1016/j.quaint.2011.02.023>

- Bona, F. 2006. Systematic position of a complete lion-like cat skull from the Eemian ossiferous rubble near Zandobbio (Bergamo, north Italy). *Rivista Italiana di Paleontologia e Stratigrafia*, 112(1):157-166.
- Boule, M. 1906. Les grands chats des cavernes. *Annales de Paléobiologie*, 1:69-95.
- Burger, J., Rosendahl, W., Loreille, O., Hemmer, H., Eriksson, T., Götherström, A., Hiller, J., Collins, M.J., Wess, T., and Alt, K.W. 2004. Molecular phylogeny of the extinct cave lion *Panthera leo spelaea*. *Molecular Phylogenetics and Evolution*, 30:841-849. <https://doi.org/10.1016/j.ympev.2003.07.020>
- Carbone, C., Mace, G.M., Roberts, S.C., and Macdonald, D.W. 1999. Energetic constraints on the diet of terrestrial carnivores. *Nature*, 402:286-288. <https://doi.org/10.1038/46266>
- Chernova, O.F., Protopopov, A.V., Boeskorov, G.G., Pavlov, I.S., Plotnikov, V.V., and Suzuki, N. 2020. First description of the fur of two cubs of fossil cave lion *Panthera spelaea* (Goldfuss, 1810) found in Yakutia in 2017 and 2018. *Doklady Biological Sciences*, 492:93-98. <https://doi.org/10.1134/s0012496620030011>
- Christiansen, P. and Harris, J.M. 2009. Craniomandibular morphology and phylogenetic affinities of *Panthera atrox*: Implications for the evolution and paleobiology of the lion lineage. *Journal of Vertebrate Paleontology*, 29:934-945. <https://doi.org/10.1671/039.029.0314>
- Clothes, J. 2001. La grotte Chauvet. L'art des origines. Seuil, Paris.
- de Manuel, M., Barnett, R., Sandoval-Velasco, M., Yamaguchi, N., Garrett Vieira, F., Zepeda Mendoza, M.L., Liu, S., Martin, M.D., Sinding, M.-H.S., Mak, S.S.T., Carøe, C., Liu, S., Guo, C., Zheng, J., Zazula, G., Baryshnikov, G., Eizirik, E., Koepfli, K.-P., Johnson, W.E., Antunes, A., Sicheritz-Ponten, T., Gopalakrishnan, S., Larson, G., Yang, H., O'Brien, S.J., Hansen, A.J., Zhang, G., Marques-Bonet, T., and Gilbert, M.T.P. 2020. The evolutionary history of extinct and living lions. *Proceedings of the National Academy of Sciences*, 117(20):10927-10934. <https://doi.org/10.1073/pnas.1919423117>
- Diedrich, C.G. 2008. The holotypes of the upper Pleistocene *Crocuta crocuta spelaea* (Goldfuss, 1823: Hyaenidae) and *Panthera leo spelaea* (Goldfuss, 1810: Felidae) of the Zoolithen Cave hyena den (South Germany) and their palaeo-ecological interpretation. *Zoological Journal of the Linnean Society*, 154:822-831. <https://doi.org/10.1111/j.1096-3642.2008.00425.x>
- Diedrich, C.G. 2009. Steppe lion remains imported by Ice Age spotted hyenas into the Late Pleistocene Perick Caves hyena den in northern Germany. *Quaternary Research*, 71:361-374. <https://doi.org/10.1016/j.yqres.2008.12.006>
- Diedrich, C.G. 2011a. Late Pleistocene *Panthera leo spelaea* (Goldfuss 1810) skeletons from the Czech Republic (Central Europe); their pathological cranial features and injuries resulting from intraspecific fights, conflicts with hyenas, and attacks on cave bears. *Bulletin of Geosciences*, 86:817-840. <https://doi.org/10.3140/bull.geosci.1263>
- Diedrich, C.G. 2011b. Late Pleistocene steppe lion *Panthera leo spelaea* (Goldfuss 1810) footprints and bone records from open air sites in northern Germany – Evidence of hyena-lion antagonism and scavenging in Europe. *Quaternary Science Reviews*, 30:1883-1906. <https://doi.org/10.1016/j.quascirev.2011.03.006>
- Diedrich, C.G. 2011c. The largest European lion *Panthera leo spelaea* (Goldfuss 1810) population from the Zoolithen Cave, Germany: specialised cave bear predators of Europe. *Historical Biology*, 23(2-3):271-311. <https://doi.org/10.1080/08912963.2010.546529>
- Diedrich, C.G. 2012. Cave bear killers and scavengers from the last ice age of central Europe: Feeding specializations in response to the absence of mammoth steppe fauna from mountainous regions. *Quaternary International*, 255:59-78. <https://doi.org/10.1016/j.quaint.2011.06.048>
- Diedrich, C.G. and Rathgeber, T. 2012. Late Pleistocene steppe lion *Panthera leo spelaea* (Goldfuss 1810) skeleton remains of the Upper Rhine Valley (SW Germany) and contributions to their sexual dimorphism, taphonomy and habitus. *Historical Biology*, 24:1-28. <https://doi.org/10.1080/08912963.2010.549943>
- Efimenko, P.P. 1958. Kostenki I. Akademiya nauk SSSR, Moscow. (In Russian)
- Ersmark, E., Orlando, L., Sandoval-Castellanos, E., Barnes, I., Barnett, R., Stuart, A., Lister, A., and Dalén, L. 2015. Population demography and genetic diversity in the Pleistocene cave lion. *Open Quaternary*, 1(4):1-15. <https://doi.org/10.5334/oq.aa>
- Gross, C. 1992. Das Skelett des Höhlenlöwen (*Panthera leo spelaea* Goldfuss, 1810) aus Siegsdorf/Ldkr. Traunstein im Vergleich mit anderen Funden aus Deutschland und den Niederlanden. Unpublished PhD Thesis, Tierärztlichen Fakultät der Ludwig-Maximilians-Universität, München, Germany.

- Guthrie, R.D. 1990. Frozen Fauna of the Mammoth Steppe: The Story of Blue Babe. The University of Chicago Press, London.  
<https://doi.org/10.7208/chicago/9780226159713.001.0001>
- Hankó, E.P. and Korsós, Z. 2007. Pleisztocén oroszlánok fog- és állkapocs-morfológiai jellegeinek kladisztyikus analízise. Állattano Közlemények, 92(1):39-51.
- Hemmer, H. 1967. Fossilbelege zur Verbreitung und Artgeschichte des Löwen, *Panthera leo* (Linné, 1758). Säugetierkundliche Mitteilungen, 15:283-300.
- Hemmer, H. 1974. Untersuchungen zur Stammesgeschichte der Pantherkatzen (Pantherinae), Teil III. Zur Artgeschichte des Löwen, *Panthera (Panthera) leo* (Linnaeus 1758). Veröffentlichungen der Zoologischen Staatssammlung München, 17:167-280.
- Hemmer, H. 2011. The story of the cave lion – *Panthera leo spelaea* (Goldfuss, 1810) – a review. Quaternaire, Hors-série 4:201-208.
- Jelínek, J. 1972. Das grosse Bilderlexikon des Menschen in der Vorzeit. Bertelsmann-Gutersloh, Berlin, München.
- Kirillova, I.V., Tiunov, A.V., Levchenko, V.A., Chernova, O.F., Yudin, V.G., Bertuch, F., and Shidlovskiy, F.K. 2015. On the discovery of a cave lion from the Malyi Anyui River (Chukotka, Russia). Quaternary Science Reviews, 117:135-151.  
<https://doi.org/10.1016/j.quascirev.2015.03.029>
- Kitchener, A.C., Breitenmoser-Wursten, C., Eizirik, E., Gentry, A., Werdelin, L., Wilting, A., Yamaguchi, N., Abramov, A.V., Christiansen, P., Driscoll, C., Duckworth, J.W., Johnson, W., Luo, S.-J., Meijaard, E., O'Donoghue, P., Sanderson, J., Seymour, K., Bruford, M., Groves, C., Hoffmann, M., Nowell, K., Timmons, Z., and Tobe, S. 2017. A revised taxonomy of the Felidae. The final report of the Cat Classification Task Force of the IUCN/SSC Cat Specialist Group. Cat News, Special Issue 11:1-80.
- Kurtén, B. 1965. The Pleistocene Felidae of Florida. Bulletin of Florida State Museum, 9:215-273.
- Kurtén, B. 1968. Pleistocene Mammals of Europe. Weidenfeld and Nicolson, London.  
<https://doi.org/10.4324/9781315126470>
- Kurtén, B. 1985. The Pleistocene lion of Beringia. Annales Zoologici Fennici, 22:117-121.
- Kurtén, B. and Poulianov, A.N. 1977. New stratigraphic and faunal material from Petralona Cave, with special reference to the Carnivora. Anthropos, 4:47-130.
- Lewis, M., Pacher, M., and Turner, A. 2010. The larger Carnivora of the West Runton Freshwater Bed. Quaternary International, 228(1-2):116-135.  
<https://doi.org/10.1016/j.quaint.2010.06.022>
- Manthi, F.K., Brown, F.H., Plavcan, M.J., and Werdelin, L. 2017. Gigantic lion, *Panthera leo*, from the Pleistocene of Natodomeri, eastern Africa. Journal of Paleontology, 92(2):305-312.  
<https://doi.org/10.1017/jpa.2017.68>
- Marciszak, A., Schouwenburg, C., and Darga, R. 2014. Decreasing size process in the cave (Pleistocene) lion *Panthera spelaea* (Goldfuss, 1810) evolution – A review. Quaternary International, 339-340:245-257. <https://doi.org/10.1016/j.quaint.2013.10.008>
- Marciszak, A., Schouwenburg, C., Gornig, W., Lipecki, G., and Mackiewicz, P. 2019. Morphometric comparison of *Panthera spelaea* (Goldfuss, 1810) from Poland with the lion remains from Eurasia over the last 700 ka. Quaternary Science Reviews, 223:105950.  
<https://doi.org/10.1016/j.quascirev.2019.105950>
- Marciszak, A., Lipecki, G., Pawłowska, K., Jakubowski, G., Ratajczak-Skrzatek, U., Zarzecka-Szubińska, K., and Nadachowski, A. 2021. The Pleistocene lion *Panthera spelaea* (Goldfuss, 1810) from Poland – a review. Quaternary International, 605-606: 213-240.  
<https://doi.org/10.1016/j.quaint.2020.12.018>
- Martin, L.D. and Gilbert, B.M. 1978. An American lion, *Panthera atrox*, from natural trap cave, north central Wyoming. Contributions to Geology, 16(2):95-101.
- Matheus, P., Guthrie, R.D., and Kunz, M.L. 2003. Predator-Prey links in Pleistocene East Beringia: evidence from stable isotopes. 3rd International Mammoth Conference, Dawson City, Yukon Territory.
- Mazák, J.H. 2004. On the sexual dimorphism in the skull of the tiger (*Panthera tigris*). Mammalian Biology, 69:392-400. <https://doi.org/10.1078/1616-5047-00161>
- Mazák, J.H. 2010. Geographical variation and phylogenetics of modern lions based on craniometric data. Journal of Zoology, 281:194-209.  
<https://doi.org/10.1111/j.1469-7998.2010.00694.x>

- Mazák, V. 1980. Zvířata celého světa 7. Velké kočky a gepardi. Státní zemědělské nakladatelství, Praha.
- Merriam, J.C. and Stock, C. 1932. The Felidae of Rancho La Brea. Carnegie Institution of Washington Publications, 442:1-227.
- Miththapala, S. 1992. Genetic and morphological variation in the leopard (*Panthera pardus*): a geographically widespread species. Unpublished PhD Thesis, University of Florida, Gainesville, USA.
- Ovodov, N.D. and Zaika, A.L. 2008. Cherep peshchernogo lva (*Panthera spelaea* Goldfuss, 1810) iz prieniseiskoi Sibiri. Faunae and Florae of Northern Eurasia in the Late Cenozoic, Institute of Plant and Animal Ecology RAS, Yekaterinburg. (In Russian)
- Rohland, N., Pollack, J.L., Nagel, D., Beauval, C., Airiaux, J., Pääbo, S., and Hofreiter, M. 2005. The Population History of Extant and Extinct Hyenas. *Molecular Biology and Evolution*, 22(12):2435-2443. <https://doi.org/10.1093/molbev/msi244>
- Sabol, M. 2011. Masters of the lost world: A hypothetical look at the temporal and spatial distribution of lion-like felids. *Quaternaire, Hors-série* 4:229-236.
- Sabol, M. 2014. *Panthera fossilis* (Reichenau, 1906) (Felidae, Carnivora) from Za Hájovnou Cave (Moravia, the Czech Republic): a fossil record from 1987-2007. *Sborník Národního Muzea v Praze – Acta Musei Nationalis Pragae, Ser. B*, 70(1-2):59-70. <https://doi.org/10.14446/amnp.2014.59>
- Sabol, M., Gullár, J., and Horvát, J. 2018. Montane record of the late Pleistocene *Panthera spelaea* (Goldfuss, 1810) from the Západné Tatry Mountains (northern Slovakia). *Journal of Vertebrate Paleontology*, 38(3):e1467921. <https://doi.org/10.1080/02724634.2018.1467921>
- Sakamoto, M. and Ruta, M. 2012. Convergence and Divergence in the Evolution of Cat Skulls: Temporal and spatial Patterns of Morphological Diversity. *PloS ONE*, 7(7):e39752. <https://doi.org/10.1371/journal.pone.0039752>
- Sala, B. 1990. *Panthera leo fossilis* (v. Reichenau, 1906) (Felidae) de Isernia la Pineta (Pléistocène moyen inférieur d'Italie). *Geobios*, 23(2):189-194. [https://doi.org/10.1016/s0016-6995\(06\)80051-3](https://doi.org/10.1016/s0016-6995(06)80051-3)
- Salis, A.T., Bray, S.C.E., Lee, M.S.Y., Heiniger, H., Barnett, R., Burns, J.A., Doronichev, V., Fedje, D., Golovanova, L., Harington, C.R., Hockett, B., Kosintsev, P., Lai, X., Mackie, Q., Vasiliev, S., Weinstock, J., Yamaguchi, N., Meachen, J., Cooper, A., and Mitchell, K.J. 2021. Lions and brown bears colonized North America in multiple synchronous waves of dispersal across the Bering Land Bridge. *Molecular Ecology*, 00:1-15. <https://doi.org/10.1111/mec.16267>
- Schouwenburg, C., Darga, R., and Rosendahl, W. 2009. De grottenleeuw, *Panthera leo spelaea* (Goldfuss 1810), uit Siegsdorf, Duitsland. *Cranium*, 26(1):31-39.
- Schütt, G. 1969. Untersuchungen am Gebiss von *Panthera leo fossilis* (v. Reichenau, 1906) und *Panthera leo spelaea* (Goldfuss, 1810). *Neues Jahrbuch für Geologie und Paläontologie, Abhandlungen* 134(2):192-220.
- Schütt, G. and Hemmer, H. 1978. Zur Evolution des Löwen (*Panthera leo* L.) im europäischen Pleistozän. *Neues Jahrbuch für Geologie und Paläontologie, Mitteilungen* 4:228-255.
- Simpson, G.G. 1941. Large Pleistocene felines of North America. *American Museum of Natural History Novitates*, 1136:1-27. <https://hdl.handle.net/2246/2262>
- Sotnikova, M.V. and Foronova, I.V. 2014. First Asian record of *Panthera (Leo) fossilis* (Mammalia, Carnivora, Felidae) in the Early Pleistocene of Western Siberia, Russia. *Integrative Zoology*, 9:517-530. <https://doi.org/10.1111/1749-4877.12082>
- Sotnikova, M. and Nikolskiy, P. 2006. Systematic position of the cave lion *Panthera spelaea* (Goldfuss) based on cranial and dental characters. *Quaternary International*, 142-143:218-228. <https://doi.org/10.1016/j.quaint.2005.03.019>
- Stanton, D.W.G., Alberti, F., Plotnikov, V., Androsov, S., Grigoriev, S., Fedorov, S., Kosintsev, P., Nagel, D., Vartanyan, S., Barnes, I., Barnett, R., Ersmark, E., Döppes, D., Germonpré, M., Hofreiter, M., Rosendahl, W., Skoglund, P., and Dalén, L. 2020. Early Pleistocene origin and extensive intra-species diversity of the extinct cave lion. *Scientific Reports*, 10:12621. <https://doi.org/10.1038/s41598-020-69474-1>
- Stuart, A.J. and Lister, A.M. 2011. Extinction chronology of the cave lion *Panthera spelaea*. *Quaternary Science Reviews*, 30:2329-2340. <https://doi.org/10.1016/j.quascirev.2010.04.023>
- Terzea, E. 1965. *Panthera spelaea* (Goldf.) în pleistocenul superior din România. *Lucrările Institutului de Speleologie „Emil Racovită“*, 4:251-281.

- Thenius, E. 1972. Die Feliden (Carnivora) aus dem Pleistozän von Stránská skála, p. 121-135. In Musil, R. (ed.), Stránská skála I 1910-1945. Studia Musei Moraviae – Anthropos 20(N. S. 12), Brno.
- Turner, A. 1984. Dental sex dimorphism in European lions (*Panthera leo* L.) of the Upper Pleistocene: palaeoecological and palaeoethological implications. Annales Zoologici Fennici, 21:1-8.
- Vereshchagin, N.K. 1971. Peshchernyi lev i ego istoria v Golarktike i v predelakh SSSR. Trudy Zoologicheskogo instituta, 49:123-199. (In Russian)
- von Koenigswald, W. and Schmitt, E. 1987. Eine pathologisch veränderte Lowentibia aus dem Jungpleistozän der nordlichen Oberrheinebene. Natur und Museum, 117(9):272-277.
- Westbury, M.V., Hartmann, S., Barlow, A., Preick, M., Ridush, B., Nagel, D., Rathgeber, T., Ziegler, R., Baryshnikov, G., Sheng, G., Ludwig, A., Wiesel, I., Dalen, L., Bibi, F., Werdelin, L., Heller, R., and Hofreiter, M. 2020. Hyena paleogenomes reveal a complex evolutionary history of cross-continental gene flow between spotted and cave hyena. Science Advances, 6(11): eaay0456. <https://doi.org/10.1126/sciadv.aay0456>
- Wiszniewska, T. 1978. *Panthera spelaea* (Goldfuss) z jaskini Niedźwiedziej w Kletnie. Acta Universitatis Wratislaviensis, No. 311, Studia geograficzne, 24:113-141.
- Wurm, A. 1912. Beiträge zur Kenntnis der diluvialen Säugetierfauna von Mauer an der Elsenz (bei Heidelberg). I. *Felis leo fossilis*. Jahres-Berichte und Mitteilungen des Oberrheinischen geologischen Vereines, Neue Folge, Bd. 2:77-102.
- Yamaguchi, N., Cooper, A., Werdelin, L., and Macdonald, D.W. 2004. Evolution of the mane and group-living in the lion (*Panthera leo*): a review. Journal of the Zoological Society of London, 263:329-342. <https://doi.org/10.1017/s0952836904005242>

**APPENDIX 1.**

Dataset of analyzed lion-like felid crania used for the analyses mentioned in the paper.

Site and Institutional Number of the Skull	Standard Nomen	Original Nomen	Sex	Ontogenetic Age	Greatest Cranial Length (L)	Palatal Length (LP)
Ichetucknee (UF 9076)	<i>atrox</i>	<i>atrox</i>	male	adult	404.0	180.0
Natural Trap Cave (KUVP 31417)	<i>atrox</i>	<i>atrox</i>	female	adult	315.5	-
Rancho la Brea (No. 20049)	<i>atrox</i>	<i>atrox</i>	male	adult	447.5	158.5
Rancho la Brea (No. 2900-3)	<i>atrox</i>	<i>atrox</i>	male	adult	458.0	134.4
Rancho la Brea (No. 2900-4)	<i>atrox</i>	<i>atrox</i>	female	adult	325.8	126.1
Rancho la Brea (No. 2900-6)	<i>atrox</i>	<i>atrox</i>	female	adult	310.3	121.7
Rancho la Brea (No. 2900-7)	<i>atrox</i>	<i>atrox</i>	female	adult	373.5	140.8
Rancho la Brea (No. 2900-8)	<i>atrox</i>	<i>atrox</i>	male	adult	391.9	136.5
Rancho la Brea (No. 2900-9)	<i>atrox</i>	<i>atrox</i>	male	adult	429.5	148.0
Mauer	<i>fossilis</i>	<i>fossilis</i>	male	adult	442.0	-
Azé I-3 (AZE.K.13.29)	<i>fossilis</i>	<i>fossilis</i>	male	prime adult	417.4	181.0
Romain-la-Roche (FEL.03, specimen 3)	<i>intermedia</i>	<i>spelaea</i>	female	adult	364.8	161.5
Vence	<i>intermedia</i>	<i>spelaea</i>	male	adult	354.0	-
Edingen (SMNS no. 6617.1.9.72.2)	<i>intermedia</i>	<i>spelaea</i>	male	adult	440.0	-
Niedźwiedzia (K-111)	<i>intermedia</i>	<i>primitive spelaea</i>	male	adult	414.0	-
San (Coll. Nr NKM-00664)	<i>intermedia</i>	<i>primitive spelaea</i>	male	adult	451.0	200.0
Petalona (PEC 90)	<i>intermedia</i>	<i>fossilis-spelaea</i>	male	adult	416.0	178.5
Bottrop (EHQB No. MBOT 6349/19a-b)	<i>spelaea</i>	<i>spelaea</i>	male	adult	380.0	-
Huttenheim (SMNS no. 6816.5.6.73.1)	<i>spelaea</i>	<i>spelaea</i>	male	adult	375.0	-
Perickhöhlen (BMNH No. 28553)	<i>spelaea</i>	<i>spelaea</i>	female	adult	301.0	-
Siegsdorf	<i>spelaea</i>	<i>spelaea</i>	male	prime adult	384.0	179.0
Zoolithenhöhle (holotype; MB no. Ma.50948)	<i>spelaea</i>	<i>spelaea</i>	male	adult	402.0	-
Zoolithenhöhle (MB no. Ma.48155.1)	<i>spelaea</i>	<i>spelaea</i>	male	adult	401.0	-
Zoolithenhöhle (UM-O no. BT5421)	<i>spelaea</i>	<i>spelaea</i>	male	adult	395.0	-
Zoolithenhöhle (MB no. Ma.50947)	<i>spelaea</i>	<i>spelaea</i>	female	adult	355.0	-
Zandobbio (MCSNB 5127)	<i>spelaea</i>	<i>spelaea</i>	female	adult	324.2	-
Brno (Anthropos specimen)	<i>spelaea</i>	<i>spelaea</i>	female	adult	-	-
Sloup (Vienna specimen; NHMV No. 1885/0014/4302)	<i>spelaea</i>	<i>spelaea</i>	male	adult	393.0	-
Sloup (Anthropos specimen)	<i>spelaea</i>	<i>spelaea</i>	male	prime adult	375.0	-
Sloup (OK 130570)	<i>spelaea</i>	<i>spelaea</i>	male	adult	386.5	170.5
Srbsko - Chlum Komín Cave (NM R-4406)	<i>spelaea</i>	<i>spelaea</i>	female	prime adult	305.0	-
Výpustek 1 (Anthropos specimen)	<i>spelaea</i>	<i>spelaea</i>	male	prime adult	412.0	-
Výpustek 3 (Anthropos specimen)	<i>spelaea</i>	<i>spelaea</i>	male	adult	-	-
Ignita	<i>spelaea</i>	<i>spelaea</i>	female	adult	333.0	-
Ursilor - level III, chamber 2, skeleton 3 (SIER no. PU/0001)	<i>spelaea</i>	<i>spelaea</i>	female	adult	302.0	-

Binagady (Caucasus) (No. 25)	<i>spelaea</i>	<i>spelaea</i>	female	adult	310.0	128.0
Desna (No. A-34)	<i>spelaea</i>	<i>spelaea</i>	male	adult	375.0	-
Isa River (South Ural) (No. 1417)	<i>spelaea</i>	<i>spelaea</i>	male	adult	355.0	153.0
Isa River (South Ural) (No. 9048)	<i>spelaea</i>	<i>spelaea</i>	male	adult	380.0	166.0
Kondakovka (K-1)	<i>spelaea</i>	<i>vereshchagini</i>	male	prime adult	345.1	-
Mokhokho (ZIN 29398)	<i>spelaea</i>	<i>vereshchagini</i>	female	adult	303.0	147.0
Uzhur (Central Siberia) (KKM 11938)	<i>spelaea</i>	<i>spelaea</i>	male	senile adult	350.0	170.0
Medvedia Cave in Western Tatras (P 14359)	<i>spelaea</i>	<i>spelaea</i>	male	prime adult	437.0	186.2
Medvedia Cave in Western Tatras (P 04696)	<i>spelaea</i>	<i>spelaea</i>	female	adult	349.0	-
western India (SNM-PM 1701)	<i>leo persica</i>	<i>leo</i>	male	adult	378.2	157.8
Africa (SNM-PM C1521)	<i>leo</i>	<i>leo</i>	female	adult	302.5	138.7
Africa (Anthropos specimen)	<i>leo</i>	<i>leo</i>	female	prime adult	302.1	141.5
Senegal (Nr 986)	<i>leo</i>	<i>leo</i>	male	prime adult	334.3	147.4
Zambezi - Zambia (NMW 1241)	<i>leo</i>	<i>leo</i>	male	adult	344.0	147.6
Chad (NMW 4234/B/4694)	<i>leo</i>	<i>leo</i>	male	prime adult	366.7	167.0
Tanzania (NMW 5489/B/5124)	<i>leo</i>	<i>leo</i>	male	prime adult	348.6	143.4
Cameroon (NMW 32819)	<i>leo</i>	<i>leo</i>	female	adult	300.4	136.3

Site and Institutional Number of the Skull	Medial Length of Nasals (LMN)	Lateral Length of Nasals (LLN)	Greatest Nasal Width (BN)	Snout Width (BS)	Width across Zygomatic Arches (BZ)	Greatest Neurocranial Width (BNC)
Ichetucknee (UF 9076)	94.0	-	61.3	-	251.0	-
Natural Trap Cave (KUVP 31417)	77.8	82.1	51.9	95.6	212.0	-
Rancho la Brea (No. 20049)	104.5	-	69.9	127.3	276.3	-
Rancho la Brea (No. 2900-3)	-	-	73.0	141.4	294.0	-
Rancho la Brea (No. 2900-4)	82.7	-	53.2	98.3	225.2	-
Rancho la Brea (No. 2900-6)	79.2	-	51.4	98.0	205.7	-
Rancho la Brea (No. 2900-7)	90.9	-	63.2	111.8	235.3	-
Rancho la Brea (No. 2900-8)	96.0	-	63.9	116.9	245.0	-
Rancho la Brea (No. 2900-9)	101.6	-	67.0	122.8	296.5	-
Mauer	-	-	-	113.0	300.0	-
Azé I-3 (AZE.K.13.29)	104.6	120.5	62.2	112.3	283.4	111.3
Romain-la-Roche (FEL.03, specimen 3)	-	-	44.0	94.0	225.6	92.0
Vence	80.8	92.4	61.6	100.0	241.0	-
Edingen (SMNS no. 6617.1.9.72.2)	127.3	131.8	77.3	136.4	281.8	-
Niedźwiedzia (K-111)	-	-	63.0	90.0	272.0	-
San (Coll. Nr NKM-00664)	-	-	55.2	138.0	300.0	96.5
Petalona (PEC 90)	60.0	62.0	46.0	115.2	-	98.7
Bottrop (EHQB No. MBOT 6349/19a-b)	96.9	119.2	67.1	111.8	-	-
Huttenheim (SMNS no. 6816.5.6.73.1)	95.9	106.1	69.4	110.2	244.9	-
Perickhöhlen (BMNH No. 28553)	-	-	53.1	106.1	-	-
Siegsdorf	100.0	113.3	58.0	106.0	250.5	-
Zoolithenhöhle (holotype; MB no. Ma.50948)	-	-	-	131.4	285.7	-
Zoolithenhöhle (MB no. Ma.48155.1)	109.1	118.2	100.0	136.4	-	-

Zoolithenhöhle (UM-O no. BT5421)	95.5	109.1	81.8	127.2	-	-
Zoolithenhöhle (MB no. Ma.50947)	81.8	100.0	72.7	109.1	263.6	-
Zandobbio (MCSNB 5127)	81.8	104.6	65.9	-	225.1	93.9
Brno (Anthropos specimen)	-	-	-	-	-	96.5
Sloup (Vienna specimen; NHMV No. 1885/0014/4302)	100.0	109.1	86.4	113.6	251.0	-
Sloup (Anthropos specimen)	81.8	100.0	63.6	100.0	232.0	-
Sloup (OK 130570)	-	-	65.4	112.0	-	111.6
Srbsko - Chlum Komín Cave (NM R-4406)	-	-	52.8	91.0	199.7	94.5
Výpustek 1 (Anthropos specimen)	-	-	60.6	118.2	-	129.5
Výpustek 3 (Anthropos specimen)	82.0	97.0	54.0	101.1	235.4	106.4
Igrita	77.7	92.9	55.1	101.5	232.0	-
Ursilor - level III, chamber 2, skeleton 3 (SIER no. PU/0001)	-	79.1	50.3	86.3	215.7	-
Binagady (Caucasus) (No. 25)	-	89.0	52.0	80.0	185.0	-
Desna (No. A-34)	-	107.0	-	111.0	240.0	-
Isa River (South Ural) (No. 1417)	-	94.0	62.0	101.0	244.0	-
Isa River (South Ural) (No. 9048)	-	100.0	61.0	110.0	244.0	-
Kondakovka (K-1)	-	92.3	69.2	103.0	249.0	-
Mokhokho (ZIN 29398)	68.2	72.9	52.9	87.0	198.1	-
Uzhur (Central Siberia) (KKM 11938)	86.5	93.3	65.5	109.5	234.0	-
Medvedia Cave in Western Tatras (P 14359)	108.3	119.6	66.5	117.8	-	118.0
Medvedia Cave in Western Tatras (P 04696)	86.7	107.0	58.6	99.8	-	100.6
western India (SNM-PM 1701)	99.6	114.3	63.0	114.2	272.0	118.0
Africa (SNM-PM C1521)	66.0	84.0	49.5	88.8	206.0	97.5
Africa (Anthropos specimen)	73.6	86.8	57.6	87.1	198.2	89.0
Senegal (Nr 986)	80.8	100.2	56.4	86.4	223.0	100.0
Zambezi - Zambia (NMW 1241)	85.0	103.2	49.1	95.6	220.2	106.4
Chad (NMW 4234/B/4694)	85.3	103.8	55.2	98.0	254.0	105.5
Tanzania (NMW 5489/B/5124)	85.0	104.8	51.1	94.6	230.0	104.5
Cameroon (NMW 32819)	81.7	98.8	45.3	85.2	201.0	97.6

Site and Institutional Number of the Skull	Mastoid Width (BM)	Interorbital Width (IOB)	Postorbital Width/ Constriction (POC)	Greatest Diameter of the Auditory Bullae (LAB)	Profile Depth	Profile Depth of Assumed Straight Cranial
Ichetucknee (UF 9076)	146.0	86.5	73.0	-	139.4	
Natural Trap Cave (KUVP 31417)	133.6	86.4	64.8	-	110.7	
Rancho la Brea (No. 20049)	158.2	93.5	84.8	30-Aug	146.9	
Rancho la Brea (No. 2900-3)	173.6	-	-	29-Jun	144.8	
Rancho la Brea (No. 2900-4)	132.7	75.3	72.0	23.0	117.2	
Rancho la Brea (No. 2900-6)	126.7	68.8	70.7	22.0	102.1	
Rancho la Brea (No. 2900-7)	138.2	83.3	78.8	22-Mar	116.5	
Rancho la Brea (No. 2900-8)	144.8	83.6	75.5	28.0	124.6	
Rancho la Brea (No. 2900-9)	-	98.3	85.0	29.2	142.6	
Mauer	166.6	88.2	69.0	-	139.3	147.3

Azé I-3 (AZE.K.13.29)	162.5	93.0	95.3	52.5	130.4	141.6
Romain-la-Roche (FEL.03, specimen 3)	137.9	79.4	71.0	41.8	145.4	150.6
Vence	115.4	92.4	77.0	-	112.8	120.3
Edingen (SMNS no. 6617.1.9.72.2)	172.7	109.1	81.8	-	156.8	163.2
Niedźwiedzia (K-111)	161.2	84.0	85.1	-	146.1	155.8
San (Coll. Nr NKM-00664)	176.0	108.0	93.8	55.8	141.9	148.1
Petalona (PEC 90)	-	89.4	70.9	-	142.1	147.2
Bottrop (EHQB No. MBOT 6349/19a-b)	134.1	96.9	-	-	131.5	
Huttenheim (SMNS no. 6816.5.6.73.1)	-	89.8	85.7	-	120.8	
Perickhöhlen (BMNH No. 28553)	138.8	81.6	77.6	-	104.4	
Siegsdorf	152.0	76.8	64.5	46.0	125.8	
Zoolithenhöhle (holotype; MB no. Ma.50948)	166.7	108.6	94.3	-	137.5	142.8
Zoolithenhöhle (MB no. Ma.48155.1)	177.3	127.3	100.0	-	145.8	
Zoolithenhöhle (UM-O no. BT5421)	163.6	104.6	90.9	-	135.8	
Zoolithenhöhle (MB no. Ma.50947)	154.6	100.0	90.9	-	119.7	
Zandobbio (MCSNB 5127)	130.1	71.5	62.6	46.7	109.9	
Brno (Anthropos specimen)	122.7	60.5	61.3	33.7	-	
Sloup (Vienna specimen; NHMV No. 1885/0014/4302)	-	76.0	90.9	-	112.3	
Sloup (Anthropos specimen)	-	77.0	81.8	-	117.3	128.7
Sloup (OK 130570)	162.4	-	65.2	-	140.1	
Srbsko - Chlum Komín Cave (NM R-4406)	130.6	92.5	65.1	44.2	104.2	
Výpustek 1 (Anthropos specimen)	160.4	93.0	78.2	-	-	
Výpustek 3 (Anthropos specimen)	152.2	71.2	63.8	43.7	-	
Ignita	134.0	70.4	56.0	-	109.2	
Ursilor - level III, chamber 2, skeleton 3 (SIER no. PU/0001)	136.6	79.1	64.7	-	107.4	
Binagady (Caucasus) (No. 25)	-	58.0	56.0	47.0	87.8	
Desna (No. A-34)	152.0	78.0	71.0	-	119.3	
Isa River (South Ural) (No. 1417)	-	73.0	66.0	48.0	120.7	
Isa River (South Ural) (No. 9048)	-	77.0	72.0	46.0	116.1	
Kondakovka (K-1)	153.0	72.0	62.0	-	112.8	121.5
Mokhokho (ZIN 29398)	124.2	58.2	59.8	-	96.9	
Uzjur (Central Siberia) (KKM 11938)	142.0	83.0	68.0	-	-	
Medvedia Cave in Western Tatras (P 14359)	163.0	86.6	75.4	51.8	131.3	
Medvedia Cave in Western Tatras (P 04696)	130.0	74.8	67.0	-	118.1	
western India (SNM-PM 1701)	143.8	84.4	70.0	46.3	126.8	131.1
Africa (SNM-PM C1521)	115.4	56.5	59.7	43.8	109.2	111.7
Africa (Anthropos specimen)	120.4	61.4	62.0	43.6	110.5	
Senegal (Nr 986)	128.0	61.8	64.8	47.5	117.4	
Zambezi - Zambia (NMW 1241)	132.0	67.4	58.6	49.7	105.5	
Chad (NMW 4234/B/4694)	137.8	69.7	60.2	54.6	108.6	
Tanzania (NMW 5489/B/5124)	130.0	68.6	64.5	47.6	109.7	
Cameroon (NMW 32819)	119.0	63.4	62.0	46.4	109.9	

Site and Institutional Number of the Skull	Cranial Profile Angle (A)	Angle B	Angle C	Cranial Profile
Ichetucknee (UF 9076)	178	142	97	0
Natural Trap Cave (KUVP 31417)	178	135	111	0
Rancho la Brea (No. 20049)	177	146	108	0
Rancho la Brea (No. 2900-3)	180	143	104	0
Rancho la Brea (No. 2900-4)	174	143	103.5	0
Rancho la Brea (No. 2900-6)	177	145.5	103	0
Rancho la Brea (No. 2900-7)	177	143	108	0
Rancho la Brea (No. 2900-8)	174	141	106	0
Rancho la Brea (No. 2900-9)	180	139	106.5	0
Mauer	170	140	88	2
Azé I-3 (AZE.K.13.29)	161	142	98	2
Romain-la-Roche (FEL.03, specimen 3)	168	-	95	2
Vence	162	140	107	2
Edingen (SMNS no. 6617.1.9.72.2)	174	136	97	1
Niedzwiedzia (K-111)	160	126	104	2
San (Coll. Nr NKM-00664)	164	130	125	2
Petalona (PEC 90)	174	138	95	1
Bottrop (EHQB No. MBOT 6349/19a-b)	180	140	107	0
Huttenheim (SMNS no. 6816.5.6.73.1)	177	141	107	0
Perickhöhlen (BMNH No. 28553)	174	136	96	0
Siegsdorf	179	140	102	0
Zoolithenhöhle (holotype; MB no. Ma.50948)	172	-	107	1
Zoolithenhöhle (MB no. Ma.48155.1)	175	140	97	0
Zoolithenhöhle (UM-O no. BT5421)	174	144	102	0
Zoolithenhöhle (MB no. Ma.50947)	170	147	99	0
Zandobbio (MCSNB 5127)	180	149	98	0
Brno (Anthropos specimen)	173	139	100	0
Sloup (Vienna specimen; NHMV No. 1885/0014/4302)	177	145	100	0
Sloup (Anthropos specimen)	165	140	111	2
Sloup (OK 130570)	175	145	100	0
Srbsko - Chlum Komín Cave (NM R- 4406)	175	134	95	0
Výpustek 1 (Anthropos specimen)	175	142	110	0
Výpustek 3 (Anthropos specimen)	173	149	98	0
Igrita	178	150	103	0
Ursilor - level III, chamber 2, skeleton 3 (SIER no. PU/0001)	>180	139	111	0
Binagady (Caucasus) (No. 25)	178	145	114	0
Desna (No. A-34)	170-180	-	109	0
Isa River (South Ural) (No. 1417)	176	149	109	0
Isa River (South Ural) (No. 9048)	173	-	106	0
Kondakovka (K-1)	160	-	100	2

Mokhokho (ZIN 29398)	178	144	103	0
Uzhur (Central Siberia) (KKM 11938)	171	139	106	0
Medvedia Cave in Western Tatras (P 14359)	176	145	104	0
Medvedia Cave in Western Tatras (P 04696)	178	131	121	0
western India (SNM-PM 1701)	170	149.5	96	1
Africa (SNM-PM C1521)	170	147	96	1
Africa (Anthropos specimen)	176	150	101	0
Senegal (Nr 986)	189	149	106	0
Zambezi - Zambia (NMW 1241)	175	144	103	0
Chad (NMW 4234/B/4694)	174	149	105	0
Tanzania (NMW 5489/B/5124)	174	151	105	0
Cameroon (NMW 32819)	187	140	100	0

Site and Institutional Number of the Skull	Standard Age (Age)	Altitude (m a.s.l.)	Source
Ichetucknee (UF 9076)	Last Glacial (Late Pleistocene, Wisconsinian)	5	Kurtén, 1965
Natural Trap Cave (KUVP 31417)	Last Glacial (Late Pleistocene, Wisconsinian, 24 000 BP)	1,700	Martin and Gilbert, 1978
Rancho la Brea (No. 20049)	Last Glacial (Late Pleistocene, Wisconsinian, 30 000 - 11 000 BP)	50	Merriam and Stock, 1932
Rancho la Brea (No. 2900-3)	Last Glacial (Late Pleistocene, Wisconsinian, 30 000 - 11 000 BP)	50	Merriam and Stock, 1932
Rancho la Brea (No. 2900-4)	Last Glacial (Late Pleistocene, Wisconsinian, 30 000 - 11 000 BP)	50	Merriam and Stock, 1932
Rancho la Brea (No. 2900-6)	Last Glacial (Late Pleistocene, Wisconsinian, 30 000 - 11 000 BP)	50	Merriam and Stock, 1932
Rancho la Brea (No. 2900-7)	Last Glacial (Late Pleistocene, Wisconsinian, 30 000 - 11 000 BP)	50	Merriam and Stock, 1932
Rancho la Brea (No. 2900-8)	Last Glacial (Late Pleistocene, Wisconsinian, 30 000 - 11 000 BP)	50	Merriam and Stock, 1932
Rancho la Brea (No. 2900-9)	Last Glacial (Late Pleistocene, Wisconsinian, 30 000 - 11 000 BP)	50	Merriam and Stock, 1932
Mauer	Cromerian (MIS 13 or MIS 14-15)	145	Wurm, 1912; Marciszak et al., 2019
Azé I-3 (AZE.K.13.29)	Holsteinian (MIS 11, previously Saalian, today rather Holsteinian)	275	Argant, 1988; Argant and Brugal, 2017
Romain-la-Roche (FEL.03, specimen 3)	Saalian (MIS 6, 160 k.y.a.)	420	Argant, 2010; Argant and Brugal, 2017
Vence	Saalian (late Middle / Late Pleistocene?)	300	Boule, 1906
Edingen (SMNS no. 6617.1.9.72.2)	Eemian (Late Pleistocene, ? between MIS 6 and MIS 5)	100	Diedrich and Rathgeber, 2012
Niedźwiedzia (K-111)	Eemian (Late Pleistocene, Late Pleniglacial to Late Glacial)	687	Wiszniewska, 1978; Barycka, 2008
San (Coll. Nr NKM-00664)	Eemian (Late Pleistocene, ? between MIS 6 and MIS 5)	750	Marciszak et al., 2014
Petalona (PEC 90)	Saalian (late Middle Pleistocene?)	254	Baryshnikov and Tsoukala, 2010
Bottrop (EHQB No. MBOT 6349/19a-b)	Last Glacial (35 000 - 42 000 BP)	35	Diedrich, 2011b

Huttenheim (SMNS no. 6816.5.6.73.1)	Last Glacial (Late Pleistocene)	100	Diedrich and Rathgeber, 2012
Perickhöhlen (BMNHL No. 28553)	Last Glacial (75 - 35 ka BP)	250	Diedrich, 2009
Siegsdorf	Last Glacial ( $47\ 678 \pm 1689$ calBP, $46\ 308 \pm 1614$ calBP)	615	Gross, 1992; Schouwenburg et al., 2009
Zoolithenhöhle (holotype; MB no. Ma.50948)	Last Glacial (> 35 000 BP, 28 905 ± 755 BP)	455-470	Diedrich, 2008
Zoolithenhöhle (MB no. Ma.48155.1)	Last Glacial (> 35 000 BP, 28 905 ± 755 BP)	455-470	Diedrich, 2011c
Zoolithenhöhle (UM-O no. BT5421)	Last Glacial (> 35 000 BP, 28 905 ± 755 BP)	455-470	Diedrich, 2011c
Zoolithenhöhle (MB no. Ma.50947)	Last Glacial (> 35 000 BP, 28 905 ± 755 BP)	455-470	Diedrich, 2011c
Zandobbio (MCSNB 5127)	Eemian	350-470	Bona, 2006
Brno (Anthropos specimen)	Last Glacial	-	personal observation
Sloup (Vienna specimen; NHMV No. 1885/0014/4302)	Last Glacial (Late Pleistocene)	495	Diedrich, 2011a
Sloup (Anthropos specimen)	Last Glacial (Late Pleistocene)	495	Diedrich 2011a; personal observation
Sloup (OK 130570)	Last Glacial	464	personal observation
Srbsko - Chlum Komín Cave (NM R- 4406)	Last Glacial (Late Pleistocene)	240	Diedrich 2011a; personal observation
Výpustek 1 (Anthropos specimen)	Last Glacial	384	personal observation
Výpustek 3 (Anthropos specimen)	Last Glacial	384	personal observation
Igrita	Last Glacial	328	Terzea, 1965
Ursilor - level III, chamber 2, skeleton 3 (SIER no. PU/0001)	Last Glacial	482	Diedrich, 2012
Binagady (Caucasus) (No. 25)	Middle-Late Pleistocene (Q2-Q3)	-	Vereshchagin, 1971
Desna (No. A-34)	Last Glacial (Late Pleistocene, Q3)	-	Vereshchagin, 1971
Isa River (South Ural) (No. 1417)	Middle-Late Pleistocene (Q2-Q3)	100-200	Vereshchagin, 1971
Isa River (South Ural) (No. 9048)	Middle-Late Pleistocene (Q2-Q3)	100-200	Vereshchagin, 1971
Kondakovka (K-1)	Last Glacial (Late Pleistocene)	170	Sotnikova and Nikolskiy, 2006
Mokhokho (ZIN 29398)	Last Glacial (Late Pleistocene, Q3)	100	Baryshnikov and Boeskorov, 2001
Uzjur (Central Siberia) (KKM 11938)	Last Glacial (Late Pleistocene)	400-450	Ovodov and Zaika, 2008
Medvedia Cave in Western Tatras (P 14359)	Last Glacial (Last Glacial, $44\ 350 \pm 730$ yrs BC)	1,133	personal observation
Medvedia Cave in Western Tatras (P 04696)	Last Glacial (Last Glacial, > 46 000 – 47 600 BP)	1,133	personal observation
western India (SNM-PM 1701)	Recent	-	personal observation
Africa (SNM-PM C1521)	Recent	-	personal observation
Africa (Anthropos specimen)	Recent	-	personal observation
Senegal (Nr 986)	Recent	-	personal observation
Zambezi - Zambia (NMW 1241)	Recent	-	personal observation
Chad (NMW 4234/B/4694)	Recent	-	personal observation
Tanzania (NMW 5489/B/5124)	Recent	-	personal observation
Cameroon (NMW 32819)	Recent	-	personal observation